

**A REVIEW OF APPLICATION OF PRESSURE DERIVATIVE
CONCEPT TO MULTIRATE TESTS**

**A
PROJECT**

**Presented to Faculty
of the African University of Science and Technology**

**in Partial Fulfillment of the Requirements
for the Degree of**

MASTER OF SCIENCE IN PETROLEUM ENGINEERING

By

Onuh, Haruna Monday, B.Sc.

Abuja, Nigeria

December 2009

**A REVIEW OF APPLICATION OF PRESSURE DERIVATIVE
CONCEPT TO MULTIRATE TESTS**

By

Onuh, Haruna Monday

RECOMMENDED:

Chair: Prof. Djebbar Tiab

.....

Prof. Ekwere J. Peters

.....

Prof. David Ogbe

APPROVED:

Chief Academic Officer

Date: 18th December 2009

***Dedicated To My Loving Parents and Sweet Heart – Audu Tasallah
Hilda. I Love you.***

ACKNOWLEDGEMENT

First and foremost I would like to thank my parents who have been a pillar of strength through out my life. To my most adorned pearl of inestimable value, for her support and prayers for me every step of the way, I will be forever grateful for your love and guidance. For always being there for me, my love and gratitude goes to Mrs D.C. Asunugwo and Mrs Reginald Akubo, for always asking about my thesis, thereby motivating me to keep working hard. Their support has provided me the driving force in my life.

I feel a deep sense of gratitude towards my research advisor Dr. Djebbar Tiab for his support, supervision, and assistance in this project. My special thanks goes to Dr Ekwere J. Peters for his willingness to serve on my project committee. Also I am grateful to Dr. Dinh, Anh V. and Dr. Al Rbeawi, Salam J. for their cooperation and advice and excellent guides. I am sincerely in debt to them for all their guidance, inspiration, constructive criticism and scholastic advice.

The financial support from NNPC/ESSO National Post-Graduate Scholarship as a 2008/2009 Graduate Student scholar and the African University of Science and Technology are greatly acknowledged.

Special thanks to all my most cherished family and loved ones for their prayers and support. To my friends and colleagues that offered their contributions throughout my program and to this project. I am honoured meeting you all during this phase of my life

Finally, I thank God Almighty for his grace, immeasurable favour and most of all his peace throughout my program and the completion of this project. In him and through him, I have accomplished all that I set out to do. For all the blessings and guidance

without which nothing that I have achieved could have been done, I bless his name.

Onuh, Haruna Monday

AUST, Abuja

Dec, 2009

TABLE OF CONTENTS

	Page
ACKNOWLEDGMENTS	IV
LIST OF TABLES	IX
LIST OF FIGURES	X
ABSTRACT	XI
 CHAPTER ONE	
INTRODUCTION	1
1.1 Overview.....	2
1.2 Literature Review.....	4
1.3 Objectives and Scope of Work.....	6
1.4 Study Organization.....	6
 CHAPTER TWO	
THEORY FOR OIL RESERVOIRS	7
2.1 Application of Multi-Rate Test in Oil Reservoirs.....	7
2.2 Pressure-Function for a Continuously Changing Flow-Rate.....	9
2.3 Pressure-Derivative for a Continuously Changing Flow-Rate.....	10
2.4 Direct Synthesis Technique for Multi-Rate Test.....	12
2.4.1 Direct Synthesis Technique for a Continuously Changing Flow-Rate.....	12
 CHAPTER THREE	
TEST PROCEDURE AND METHODOLOGY	15
3.1 Multi-Rate Test (MRT).....	15
3.1.1 Numerical Example of MRT in an Oil Reservoir	15
3.1.1(a) Pressure Function for the MRT.....	15

3.1.1(b) Pressure Derivative for the MRT.....	16
3.2 MRT for a Continuously Changing Flow-Rate.....	17
3,2,1 Conventional Method: Cartesian Plot.....	17
3,2,2 Conventional Method: Semi-Log Plot.....	18
3,2,3 Tiab's Direct Synthesis.....	18
3.3 Three-Rate Test in an Oil Reservoir	19
3.3.1 Pressure Function for Three Rate Test.....	19
3.3.2 Pressure Derivative for Three Rate Test.....	19
3.3.3 Numerical Example for Three Rate Test in Oil Reservoir.....	20
3.3.3.1 Pressure Function for the Three Rate Test.....	20
3.3.3.2 Pressure Derivative for the Three Rate Test.....	20
3.4 Two-Rate Test in an Oil Reservoir	20
3.4.1 Pressure Function for Two Rate Test.....	22
3.4.2 Pressure Derivative for Two Rate Test.....	23
3.4.3 Tiab's Direct Synthesis for Two Rate Test.....	24
3.4.4 Numerical Example for Two Rate Test.....	24
3.4.4.1 Pressure Function for the Two Rate Test.....	25
3.4.4.2 Pressure Derivative for the Two Rate Test.....	25
3.4.4.3 Tiab's Direct Synthesis for the Two Rate Test.....	26

CHAPTER FOUR

DATA ANALYSIS, RESULTS, AND DISCUSSIONS.....	28
4.1 Introduction.....	28
4.2 Analysis for Multirate test.....	28
4.3 Analysis for Three Rate Test.....	28
4.4 Analysis for Two Rate Test.....	29
4.5 Summary.....	29

CHAPTER FIVE

SUMMARY, CONCLUSIONS AND RECOMMENDATIONS.....	30
5.1 Summary.....	30
5.2 Conclusions.....	30
5.3 Recommendations.....	31
NOMENCLATURE.....	32
REFERENCES.....	34
APPENDIX A.....	37
APPENDIX B.....	44

LIST OF TABLES

Tables	Page
3.1.1 Variable Flow Rate Drawdown Data.....	44
3.1.2 $\Delta P'_{wf}$ psi/hr and Σ Data.....	45
3.2 Two-Rate Test Data.....	45
3.3 Data for Three and Multi-Rate Test.....	46
4.1 Comparison of Results Estimated by Different Techniques for Continuously Changing Flowrates	47
4.2 Comparison of Results Estimated by Different Techniques for Constant Flowrates	47
4.3 Comparison of Results Estimated by Different Techniques for Two-Rate Test	48

LIST OF FIGURES

Figures

Page

1	Schematic Representation of a Variable Production-Rate (After Earlougher).....	37
2	Schematic Representation of a Two-Rate Test.....	37
3	Pressure-Function for a Multi-Rate Test.....	38
4	Pressure-Derivative for a Multi-Rate Test	38
5	Semi-log Plot of P_{wf} versus time for the Multi-Rate Test.....	39
6	Cartesian Plot of Normalized Pressure versus Superposition Time, X_n for the Multi-Rate Test.....	39
7	Semi-log Plot of Normalized Pressure versus Equivalent . Time, t_{eq} for the Multi-Rate Test	40
8.	Semi-log Plot of Normalized Pressure versus Time, t and Equivalent Time, t_{eq}	40
9	Log-Log Plot of Normalized Pressure and Pressure Derivative versus Producing Time for the Multi-Rate Test	41
10	Pressure-Function for the Three-Rate Test.....	41
11	Pressure-Derivative for the Three-Rate Test.....	42
12	Pressure-Function for the Two-Rate Test.....	42
13	Pressure-Derivative for the Two-Rate Test.....	43
14	Direct Synthesis for the Two-Rate Test	43

ABSTRACT

Pressure build-up data in low permeability reservoirs take too long and are usually of poor quality. A pressure buildup test is perhaps the most widely performed transient test. In pressure buildup test, a well which has been producing for some time at a constant rate is shut-in and the bottomhole pressure is measured as a function of shut-in time. It is easier to conduct and interpret than most other transient tests, but often it is not economically feasible to shut in a well with a high production rate for a buildup test. Sand producing wells are not good candidates for long pressure drawdown tests. It is often impracticable to maintain a constant rate long enough to complete a drawdown test. In these cases, a multi-rate flow test should be run instead of buildup or drawdown tests. In most cases, the well is shut-in at the surface and as a result, some of the early time pressure data may be affected by wellbore storage. Actually a well-designed multi-rate flow test may minimize the influence of wellbore storage on pressure data.

A new technique based on the pressure derivative concept is presented for interpreting a multi-rate flow test. It is shown here that a Cartesian plot of the pressure derivative data versus a time group is a straight line from which the reservoir permeability can be estimated. It is also shown that for the case of two-rate test, Tiab's Direct Synthesis technique is applicable for calculating permeability and skin. A step by step procedure is presented for interpreting a multi-rate test using pressure and pressure derivative data. This new technique is illustrated by several numerical examples.

CHAPTER 1

INTRODUCTION

1.1 Overview

Pressure transient testing techniques are an important part of reservoir and production engineering. From the analysis of the pressure tests, the reservoir model can be recognized and the reservoir properties can be obtained. In order to determine such characteristics, drawdown and Buildup tests are performed. But to run successful pressure tests, many requirements have to be satisfied. For instance, pressure buildup analysis requires that:

(1) The well be shut in for a sufficient period of time Δt and (2) The producing time, during the last constant rate prior to shut in, be four times longer than the total shut in time in order to obtain actual reservoir response.

Because we need to shut the well in, the pressure build up test is uneconomical both for high production wells and tight formations due to income loss. Drawdown tests require that: (1) The well be shut in long enough, before the test is run to reach reservoir static pressure. and (2) The flowrate be maintained constant during the entire test, which is quite difficult to achieve in practice. Pressure drawdown tests are not suitable for sand-producing wells.

Consequently, in order to overcome the drawbacks of the conventional single rate tests, a Multirate flow test should be run instead. A Multirate test is a draw down test conducted at several production rates (fig. 1). A well designed, performed, and analysed multirate test yields the same results as a single flowrate test, reduces income loss and removes the effects of flowrate fluctuations on the resulting pressure transient responses. An additional advantage is the minimization of phase redistribution effects. Such a test may be conducted if:

1. An operator cannot afford to shut in a well for a build up test but wishes to obtain the same type of information that can be obtained from the build up test.
2. Sand production prevents shutting in the well for a build up test.
3. Phase segregation prevents the use of build up test.
4. Required to do so by a regulatory agency as in the case of gas wells.
5. Test began at a constant rate drawdown test, but the rate varied significantly during the test.

Reservoir parameters such as formation permeability, total skin factor, average reservoir pressure, and distance to a barrier if present, can be obtained from a Multirate test. In Multirate test, a well is flowed at a number of constant rates and the flowing BHP are recorded as a function of time. The constant rates should either be in increasing or decreasing order of magnitude. The effect can be modelled by considering a Multirate well to be several single rate well at same location, and each time the rate changes, a new well with rate equal to the total rate change is added to the calculation as shown in fig. 1.

1.2 Literature Review

A multi-rate test may be characterized by a series of constant flow rates, or uncontrolled variable rate. In fact, pressure build-up testing is a special type of multi-rate well test. The flow meters can aid in the design of both kinds of tests, variable or constant flow rates, and as a direct consequence more accurate analysis and results of their interpretation can be obtained. The approach presented here is based on the assumption that the system is infinite-acting and the logarithmic approximation to the line source solution of the diffusivity equation is applicable. The pressure behaviour caused by a variable flowrate is given by the principle of superposition with time.

The principle of superposition with time is used to develop a plot to determine the reservoir parameters. The principle states that adding solution to a linear differential equation results in a new solution to that differential equation but for different boundary condition. The concept of superposition entails: "Every flow rate change in a well will result in a pressure response which is independent of the pressure responses caused by other previous rate changes". This applies to single well with variable production flow rate.

Visualizing a single well as two wells located at the same point with one producing at rate q_1 from $t=0$ to $t=t_1$ and the second imaginary well producing at rate $(q_2 - q_1)$ starting at new time t_1 and continuing for a time period $(t - t_1)$ as shown in fig. 2.

Russell¹ developed a testing method for a two-rate flow test, which overcomes the drawbacks of buildup and drawdown tests. Geometrical and boundary effects can be inferred from a two-rate flow test analysis. The difficulty of the two-rate flow test is that the second flow rate must be constant. This is quite difficult to achieve in practice and a slight fluctuation of the flow rate, if not accounted for, may lead to considerably erroneous results. Selim² observed that the results obtained

from a two-rate test were sensitive to the slope of the straight line drawn according to the method proposed by Russell. Therefore, he suggested a modification of the method by returning the well to the producing rate it had prior to the test once the well had reached stable conditions. Pinson³ proposed to plot P_{wf} versus $\text{Log}(\Delta t)$ when the first flow rate lasts over a long period of time, when compared with the second flow rate time. Earlougher⁴ developed a technique for the estimation of the errors in the calculated transmissibility and skin factor, when Pinson's analysis technique is used for a two-rate flow test. These errors can be used to decide which technique should be applied. As mentioned above, in practice, it is quite difficult to maintain both first and second flow rates constant. For this reason, it is necessary to modify the two-rate flow equations. Odeh and Jones⁵ modified the procedure by removing the constant rate requirement during the second flow period. Thus, any drift in rate is taken into consideration in the calculation of results. Doyle and Sayegh⁶ presented a method to calculate average reservoir pressure, formation damage and reservoir characteristics from a three-rate transient test in gas wells. The conventional semi-log or log-log type curve matching techniques are used to analyse Multirate tests. Tiab introduced first the direct synthesis technique for interpreting pressure transient tests for a well producing at constant flowrates. This uses log-log plots of pressure and the pressure derivative versus time to compute several reservoir parameters without using the type curve matching technique.

Pressure drop at a single well is given as

$$\Delta P = \frac{141.2\mu B}{kh} \left[q_1 (P_D(r_{D1}, t_D) + S) + (q_2 - q_1) (P_D(r_{D1}, (t - t_1)_D) + S) \right] \quad (1.1)$$

In oil field units: pressure at any point or observation well at distance r from the active well is given as:

$$\Delta P = \frac{-70.6\mu B}{kh} \left[(q_1 - q_0) E_i \left(\frac{948\Phi\mu C_t r^2}{k(t - t_o)} \right) + (q_2 - q_1) E_i \left(\frac{948\Phi\mu C_t r^2}{k(t - t_1)} \right) \right] \quad (1.2)$$

The general form of this equation is given as:

$$\Delta P = \frac{141.2\mu}{kh} \sum_{i=1}^n [(qB)_i - (qB)_{i-1}] [P_D(r_{Di}, (t - t_{i-1})_D + S)] \quad (1.3)$$

In oil field units, for n constant rates this gives:

$$P_{wf} = P_i - \frac{B\mu}{0.007082kh} \sum_{i=1}^n P_{Di} \Delta q_i \quad (1.4)$$

Where $\Delta q_i = q_i - q_{i-1}$,

$q_0 = 0$

P_{Di} is determined at $t-t_{i-1}$ which is the time each rate change has been in effect, t = current time, t_{i-1} = time when rate was changed to q_i and $t_0 = 0$.

If the reservoir is infinite acting for each flow rate, then

$$P_{Di} = 0.5 \left[\ln(t_{Dwi}) - 0.80907 \right] \quad (1.5)$$

where

$$t_{Dwi} = \frac{0.0002637k(t-t_{i-1})}{\Phi\mu C_t r_w^2} \quad (1.6)$$

This implies that:

$$P_{wf} = P_i - \frac{B\mu}{2\pi kh} \sum_{i=1}^n 0.5 \left[\ln \left(\frac{k(t-t_{i-1})}{\Phi\mu C_t r_w^2} \right) + 0.80907 \right] \Delta q_i \quad (1.7)$$

Dividing through by q_n gives

$$\frac{P_i - P_{wf}}{q_n} = m' \sum_{i=1}^n \frac{q_i - q_{i-1}}{q_n} \log(t - t_{i-1}) + m' \{ \bar{S} \} \quad (1.8)$$

Division by q_n ensures that the plot in each flow period lines up to give one straight line with the same intercept.

For instance, for a three rate test,

$$@ n=1, \sum_{i=1}^n \frac{q_i - q_{i-1}}{q_n} \log(t - t_{i-1}) = \frac{q_1 - q_0}{q_1} \log(t - t_0)$$

$$@ n=2, \sum_{i=1}^n \frac{q_i - q_{i-1}}{q_n} \log(t - t_{i-1}) = \frac{q_2 - q_1}{q_2} \log(t - t_1) + \frac{q_1}{q_2} \log(t)$$

$$@ n=3, \sum_{i=1}^n \frac{q_i - q_{i-1}}{q_n} \log(t - t_{i-1}) = \frac{q_3 - q_2}{q_3} \log(t - t_2) + \frac{q_2 - q_1}{q_3} \log(t - t_1) + \frac{q_1}{q_3} \log(t)$$

A plot of $\frac{P_i - P_{wf}}{q_n}$ versus $\sum_{i=1}^n \frac{q_i - q_{i-1}}{q_n} \log(t - t_{i-1})$ gives a slope m' and intercept,

$$b=m' \left\{ \bar{S} \right\}$$

, from which, k, kh and s are obtained.

Where

$$m' = \frac{162.6B\mu}{kh} \quad (1.9)$$

$$\bar{S} = \left[\log \left(\frac{k}{\phi \mu c_t r_w^2} \right) - 3.2275 + 0.86859 s \right] \quad (1.10)$$

From equation 1.9 and 1.10,

Permeability, k and skin factor, s is obtained as follows:

$$k = \frac{162.6\mu B}{m'h}$$

$$\bar{S} = 1.1513 \left[\frac{b'}{m'} - \log \left(\frac{k}{\phi \mu c_t r_w^2} \right) + 3.2275 \right]$$

1.3 Objective of the Study

The objective of this study is to apply a new technique based on the pressure derivative concept for interpreting a multi-rate flow test. A step by step procedure is presented for interpreting a multi-rate test using pressure and pressure derivative data. This new technique is illustrated by several numerical examples.

1.4 Organization of the Study

Chapter two covers the theory of oil reservoirs, including pressure function for continuously changing flow-rates, pressure function for constant flowrate preceded by variable flow-rates, and Direct synthesis for multirate tests. Chapter Three discusses the various test scenarios encompassing multirate test, three and two rate test. It also considers the application of a pressure-function and pressure derivative methods to multirate test and application of Tiab's Direct Synthesis in two rate test. Chapter Four presents and compares the results obtained from the pressure calculations; It includes the discussion of the results and the calculations of reservoir parameters such as permeability and skin factor. Finally, Chapter Five covers the summary, conclusions of the study, and the recommendations.

CHAPTER 2

THEORY OF OIL RESERVOIRS

2.1 Application of Pressure Derivative Concept to Multi-Rate Test in Oil Reservoir

A multi rate test is difficult to interpret because both pressure and production flow rate vary with time. If both pressure and flow rate are measured, the problem can be solved by using the convolution theorem as highlighted below:

If $f(t)$ & $g(t)$ are piecewise continuous functions on $[0, \infty)$, then convolution integral of $f(t)$ & $g(t)$ is given as:

$$(f * g)(t) = \int_0^t f(t-\tau) g(\tau) d\tau = \int_0^t f(\tau) g(t-\tau) d\tau \quad (2.1)$$

Since pressure, P and flowrate, q are also time dependent, ie $P(t)$ and $q(t)$ and are piecewise continuous functions on $[0, \infty)$ as seen in multirate test, then convolution integral of $P(t)$ and $q(t)$ is given as:

$$(P * q)(t) = \int_0^t P(t-\tau) q(\tau) d\tau \quad (2.2)$$

From Duhamel's integral,

$$P(t) \approx \sum P(\tau) \cdot \Delta\tau \cdot \delta(t - \tau) \quad (2.3)$$

$$x(t) \approx \sum P(\tau) \cdot \Delta\tau \cdot q(t-\tau) \quad (2.4)$$

as $\Delta t \rightarrow 0$, and replacing summation term by integral term:

$$x(t) = \int_0^t P(\tau) q(t-\tau) d\tau = \sum P(\tau) \cdot \Delta\tau \cdot q(t-\tau) \quad (2.5)$$

In dimensionless form, the convolution integral of $P_D(t)$ and $q(t)$ is:

$$P_D = \int_0^t q_D(\tau_D) \frac{dP_D(t_D - \tau_D)}{dt_D} d\tau_D \quad (2.6)$$

Discretizing of the equation using Riemann's integral results:

$$\sum_{i=1}^n \Delta x_k \rightarrow 0 \text{ as } n \rightarrow \infty \quad (2.7)$$

This is the general form of the dimensionless pressure equation caused by variable flowrate.

$$P_D = \sum_{i=1}^n (q_{Di} - q_{Di-1}) [P_D(t_D - t_{Di-1})] \quad (2.8)$$

Where $q_{D0} = 0$, $t_{D0} = 0$ and $q_{Di} = \frac{q}{q_{ref}}$

The line source solution to the diffusivity equation for a well producing at a constant rate in an infinite acting radial system in oil field units is given as follows (assuming that the log approximation is valid)

$$P_{Dw} = 1.1513 [\log(t) + \bar{S}] \quad (2.9)$$

Where

$$\bar{S} = \left[\log \left(\frac{k}{\phi \mu c_t r_w^2} \right) - 3.2275 + 0.86859 s \right]$$

$$P_{Dw} = \frac{kh}{141.2 q_{ref} \mu B} (P_i - P_{wf})$$

and

At the wellbore, the dimensionless pressure caused by a variable flowrate during infinite acting radial flow regime is obtain by combining the discretized equation above for P_{Dw} as shown below:

$$P_{Dw} = 1.1513 \left[\sum_{i=1}^n (q_{Di} - q_{Di-1}) \log(t - t_{i-1}) + 0.8686 q_{Dn} \bar{S} - 3.227 \right] \quad (2.10)$$

In real parameters and oil field units, equation becomes:

$$\frac{P_i - P_{wf}(t)}{q_{ref}} = \frac{162.6 \mu B}{kh} \left[\sum_{i=1}^n \frac{q_i - q_{i-1}}{q_{ref}} \log(t - t_{i-1}) + 0.8686 \frac{q_n}{q_{ref}} s - 3.227 \right] \quad (2.11)$$

q_{ref} is the last flow rate at the time t_n

2.2 Pressure Function For A Continuously Changing Flow Rate.

In equation 3.23, let $q_{ref} = q_n$ and thus for practical purposes can be written as:

$$\frac{P_i - P_{wf}(t)}{q_n} = m_n \sum_{j=1}^N \left[\frac{(q_j - q_{j-1})}{q_N} \log(t - t_{j-1}) \right] + b_n \quad (2.12)$$

Equation (2.12) can also be written in the form below:

$$\frac{P_i - P_{wf}(t)}{q_n} = m_n X_n + b_n \quad (2.13)$$

where the slope = m_n , intercept = b_n and superposition time = X_n .

A plot of $\frac{P_i - P_{wf}(t)}{q_n}$ versus X_n should yield a straight line with a slope m_n , and intercept X_n during the infinite acting radial flow. Such a plot is termed a rate-normalized or multirate superposition plot. From the slope and intercept, the permeability, k and skin factor, s can be expressed as:

$$k = \frac{162.6 \mu B}{m_n h} \quad (2.14)$$

$$\bar{s} = 1.1513 \left[\frac{b_n}{m_n} - \log \left(\frac{k}{\phi \mu c_t r_w^2} \right) + 3.2275 \right] \quad (2.15)$$

In addition, equation 2.13 can be written in a different form as:

$$\frac{P_i - P_{wf}(t_n)}{q_n} = m_n \log t_{eq} + b_n \quad (2.16)$$

where $\left(\frac{q_i - q_{i-1}}{q_n} \right)^{\frac{1}{n-1}} = 10^{X_n} \quad (2.17)$

A semilog plot of $\frac{P_i - P_{wf}(t)}{q_n}$ versus either t or t_{eq} should yield a straight line

with slope m and intercept b_n . The intercept is read from the value of $\frac{P_i - P_{wf}(t)}{q_n}$

read from the straight line or its extrapolation at $t=1$ hr. The permeability and skin factor are calculated from equation 2.14 and 2.15 respectively.

2.3 Pressure Derivative Concept To Multi-Rate Tests

With the derivative approach, the time rate of change of pressure during a test period is considered for analysis. In order to emphasize the radial flow regime, the derivative is taken with respect to the logarithm of time (Bourdet et al., 1983 a).

By using the natural logarithm, the welltest derivative function can be calculated with the following central difference approximation: derivative expressed as the time derivative, multiplied by the elapsed time Δt since the beginning of the period.

$$\Delta p' = \frac{dp}{d \ln \Delta t} = \Delta t \frac{dp}{dt} \quad (2.18)$$

In dimensionless form, the function normally used to diagnose the presence of wellbore storage in the pressure data is the welltest derivative function defined as

$$P_D' = \frac{dP_D}{d \ln t_D} = t_D \frac{dP_D}{dt_D} \quad (2.19)$$

In actual variable, the welltest derivative function becomes,

$$\Delta P' = \frac{d\Delta P}{d \ln t} = t \frac{d\Delta P}{dt} = 70.6 \frac{q\mu B}{kh} = a \text{ constant} \quad (2.20)$$

The welltest derivative function can be calculated with the following central difference approximation:

$$\Delta P' = t_i \left(\frac{d\Delta P}{dt} \right)_{t_i} = t_i \left[\frac{\left(\frac{\Delta P_i - \Delta P_{i-1}}{t_i - t_{i-1}} \right) (t_{i+1} - t_i) + \left(\frac{\Delta P_{i+1} - \Delta P_i}{t_{i+1} - t_i} \right) (t_i - t_{i-1})}{(t_i - t_{i-1}) + (t_{i+1} - t_i)} \right] \quad (2.21)$$

The derivative is plotted on log-log coordinates versus Δt .

Modern analysis has been enhanced by the use of derivative plot introduced by Bourdet, Whittle, Douglas, and Pirard (1983). The advantage of derivative plot is that it is able to display in a single graph many separate characteristics that would otherwise require different plots.

Practically all wells produce at varying rates and therefore it is important that we be able to predict the pressure behaviour when rate changes.

The concept of superposition which states: "Every flow rate change in a well will result in a pressure response which is independent of the pressure responses caused by other previous rate changes".

The following equation is used to interpret a multirate test using the pressure function:

$$\frac{P_i - P_{wf}}{q_N} = m' \sum_{j=1}^N \left[\frac{(q_j - q_{j-1})}{q_N} \log(t - t_{j-1}) \right] + b' \quad (2.22)$$

where the slope is given as

$$m' = \frac{162.6 B \mu}{kh} \quad 20$$

(2.23)

and intercept as:

$$b' = m' \left[\log \left(\frac{k}{\phi \mu c_t r_w^2} \right) - 3.2275 + 0.86859 s \right] \quad (2.24)$$

The derivative with respect to

time yields:

$$\frac{\Delta P_{wf}}{\Delta t} = P'_{wf} = m'' \sum_{j=1}^N \frac{q_j - q_{j-1}}{t - t_{j-1}} \quad (2.25)$$

where the new slope is:

$$m'' = \frac{70.6 \mu B}{kh} \quad (2.26)$$

From comparing Eqs. 2.23 and 2.26:

$$m' = 2.303 m'' \quad (2.27)$$

The primary purpose of the derivative is to make sure that the appropriate straight line, for calculating k , is selected properly.

2.4 Direct Synthesis Technique For Multi-Rate Test.

2.4.1 Direct Synthesis For A Continuously Changing Flow Rate

For a continuously production flow rate, the equation governing the pressure drop at the wellbore for an infinitely acting radial flow is expressed as:

$$(P_{D_n})_r = \left(\frac{kh}{141.2 \mu B} \right) \left(\frac{(P_i - P_{wf}(t_n))}{q_n} \right) = \frac{1}{2} [\ln t_{D_{en}} + 0.80907 + 2s] \quad (2.28)$$

$$\text{where, } (t_{D_n} - t_{D_{i-1}}) \left[\frac{q_i - q_{i-1}}{q_n} \right] \quad (2.28.1)$$

$$\text{For simplicity, let } \Delta P_q = \frac{P_i - P(t_n)}{q_n} \quad (2.28.2)$$

The right hand side of equation 2.28 is the same as the dimensionless pressure for a well producing at a constant flowrate. The dimensionless pressure,

time and wellbore storage are expressed as:

$$(P_{D_n})_r = \left(\frac{kh}{141.2 \mu B} \right) \Delta P_q \quad (2.29)$$

$$C_D = \left(\frac{0.8935}{\phi h c_t r_w^2} \right) C \quad (2.30)$$

$$t_{D_{en}} = \left(\frac{0.0002637k}{\phi \mu c_t r_w^2} \right) t_{en} \quad (2.31)$$

From the numerical example (3.1), both semilog and Cartesian plots of ΔP_q versus time (t) give almost the same result.

The log-log plot of pressure versus time has a unit slope straight line as the only unique characteristic. The log-log plot of pressure derivative versus time has a unit slope straight line characteristic as well as a peak and a horizontal straight line indicating the infinite acting radial flow period. The principal characteristic of the two functions are:

- The pressure curve is characterized by a unit slope line during the early time. This corresponds to pure constant wellbore storage flow. In the case of constant wellbore storage, Van Everdingen, Agarwal et al and Wattenbarger studied this early period and developed an equation governing the sandface flowrate. From material balance, the pressure in the wellbore is directly proportional to the time during which the wellbore storage dominates the test.

Mathematically,

$$P_D = \frac{t_D}{C_D} \quad (2.32)$$

Combining equations 2.30 and 2.31 results in

$$\frac{t_D}{C_D} = [2.95 \times 10^{-4}] \left(\frac{Kh}{\mu} \right) \left(\frac{t}{C} \right) \quad (2.33)$$

Substituting equations 2.29 and 2.33 into 2.32 and solving for C gives:

$$C = \left(\frac{B}{24} \right) \left(\frac{t}{\Delta P_q} \right) \quad (2.34)$$

- The infinite acting radial flow portion of the pressure derivative is a horizontal straight line. In terms of pressure, the equation of the straight line is :

$$(P_{D_n})_r = \frac{1}{2} \left[\ln \left(\frac{t_D}{C_D} \right) + 0.80907 + \ln (C_D e^{2s}) \right] \quad (2.35)$$

The derivative of equation 2.35 with respect to natural log of $\frac{t_D}{C_D}$ is

$$\frac{t_D}{C_D} x P_{D'} = 0.5 \quad (2.36)$$

On the other hand, taking the derivative of equation 2.29 with respect to natural log of

$\frac{t_D}{C_D}$ and applying the chain rule method of differentiation results in

$$P_{D'} = \frac{\partial P_D}{\partial (t_D / C_D)} = \left(\frac{kh}{141.2 \mu B} \right) \left(\frac{\partial \Delta P_q}{\partial t} \frac{\partial t}{\partial (t_D / C_D)} \right) = \left(\frac{kh}{141.2 \mu B} \right) \left(\frac{C\mu}{2.95 \times 10^{-4} kh} \right) \Delta P'_q \quad (2.37)$$

$$\text{or } P_{D'} = \left(\frac{24C}{B} \right) \Delta P'_q \quad (2.38)$$

Substituting equation 2.33 into 2.38 results in

$$\frac{t_D}{C_D} x P_{D'} = \left(\frac{kh}{141.2 \mu B} \right) (tx \Delta P'_q)_r \quad (2.39)$$

Combining equations 2.36 and 2.39 and solving for permeability, k yields

$$k = \left(\frac{70.6 \mu B}{h (tx \Delta P'_q)_r} \right) \quad (2.40)$$

- The wellbore damage is determined from a relationship between pressure and pressure derivative during the infinite acting radial flow period. This relation can be derived by dividing equation 2.35 by 2.36 to obtain

$$\frac{(P_{D_n})_r}{[t_D / C_D] P_{D'}} = \left[\ln (t_D) + 0.80907 + 2s \right] \quad (2.41)$$

Equations 2.29, 2.30, 2.39 and 2.41 are added together to obtain the skin

$$\text{factor s, as } s = 0.5 \left[\left(\frac{(\Delta P_q)_r}{t * \Delta P'_q} \right) - \ln \left(\frac{K t_r}{\phi \mu c_t r_w^2} \right) + 7.43 \right] \quad (2.42)$$

CHAPTER 3

TEST PROCEDURE AND METHODOLOGY

3.1 Multi-Rate Test

3.1.1 Numerical Example of Multirate Test in an Oil Reservoir

A multirate test in which the oil flow rate is varied from 1320 BPD to 742 BPD during an 18.95-hr drawdown test. Tables B1 and B2 present measured pressure and flow rate data as functions of time during this test. Other known reservoir and well data are:

RESERVOIR PARAMETERS

Porosity, Φ	0.09	
Oil FVF, B_o	1.12	RB/STB
Height, h	38	ft
Compressibility, C_t	0.0000022	psi ⁻¹
Wellbore Radius, r_w	0.51	ft
Oil Viscosity, μ	4.2	cp
Eff. Wellbore Radius, r_e	∞	

The summation term is
calculated as:

$$\sum = \sum_{j=1}^N \frac{q_j - q_{j-1}}{t - t_{j-1}} \quad (3.1)$$

The superposition time is calculated as

$$X_n = \sum_{j=1}^N \left[\frac{(q_j - q_{j-1})}{q_N} \log(t - t_{j-1}) \right] \quad (3.2)$$

3.1.1(a) Pressure-Function

Fig. 3 shows the Cartesian plot of $\Delta P/q$, psi/BPD versus X_n which has two straight lines. Note that the slope of the second line is greater than that of the first, possibly indicating the presence of a fault, a lower permeability or pseudo-steady state. The slope of the first straight line is

$m_1 = 1.0525 \text{ psi/(stb/d cycle)}$, and the intercept $b_m = 2.0450 \text{ psi/(stb/d)}$.

The formation permeability is computed from Eq. 2.14 as

$$k = \frac{162.6\mu B}{m'h} = \frac{(162.6)(4.2)(1.12)}{(1.0525)(38)} = 19.12\text{md}$$

3.1.1(b) Pressure Derivatives

Fig. 4 is a Cartesian plot of $\Delta P'$, psi/hr versus Σ , BPD/hr. The straight-line of best fit of this graph indicates a slope $m'' = 0.410$ and the new permeability is calculated as follows using eqn. 2.26:

$$m'' = \frac{70.6\mu B}{kh}$$

$$k = \frac{70.6\mu B}{m''h} = \frac{(70.6)(4.2)(1.12)}{(0.410)(38)} = 21.32\text{md}$$

According to equation 3.7,

$$m' = 2.303 m'' = 2.303 \times 0.410 = 0.9442$$

Therefore, the choice of $m' = 1.0525$ psi/STB as obtained from fig 3 is incorrect. The value of permeability computed from this slope is 19.12md. The intercept, b' is obtained from figure 3 as 2.0450. and slope, $m' = 1.0525$

The skin factor, s is calculated as follows:

$$b' = m' \left[\log \left(\frac{k}{\phi \mu c_t r_w^2} \right) - 3.2275 + 0.86859 s \right]$$

$$s = 1.1513 \left[\frac{2.0450}{1.0525} - \log \left(\frac{19.12}{0.09 \times 4.2 \times 0.0000022 \times 0.51^2} \right) + 3.2275 \right] = -3.20$$

The slope of the semi-log straight line of P_{wf} versus time (Fig. 5) is -771.57psi/cycle. ie $-335.03 \times \ln(10)$;

$$\text{The permeability, } k = \frac{-162.6q\mu B}{mh} = \frac{(-162.6)(742)(4.2)(1.12)}{(-771.57)(38)} = 19.36\text{md}$$

$$s = 1.1513 \left[\frac{985.72}{771.57} - \log \left(\frac{19.36}{0.09 \times 4.2 \times 0.0000022 \times 0.51^2} \right) + 3.2275 \right] = -3.97$$

3.2 MULTI-RATE TEST FOR A CONTINUOUSLY CHANGING FLOWRATE.

Consider a drawdown test in which rate decreased continuously throughout the test. Table 3.3 shows measured pressure and flow rate data as functions of time during the test. It is observed that there exists only one pressure point for a given flowrate. Other known reservoir and well data are tabulated below:

RESERVOIR PARAMETERS

Porosity, Φ	0.2	
Oil FVF, B_o	1.3	RB/STB
Height, h	100	ft
Compressibility, C_t	0.00001	psi ⁻¹
Wellbore Radius, r_w	0.25	ft
Oil Viscosity, μ	1	cP
Eff. Wellbore Radius, r_e	∞	

In addition,

Table B3 contains summaries of normalized pressure $\frac{P_i - P_{wf}(t)}{q_n}$, superposition time X_n , equivalent time t_{eq} and derivatives.

3.2.1 Conventional Method: Cartesian Plot

A Cartesian plot of $\frac{P_i - P_{wf}(t)}{q_n}$ versus F_p is shown in fig. 6. The early time data are distorted due to wellbore storage effect. It is clear from the shape of the curve that wellbore storage effect ends at approximately 1hr 30mins. For $t > 1\text{hr } 30\text{mins}$ the plotted data lay on a straight line indicating the infinite acting radial flow. Linear regression yields a slope of straight line, $m' = 0.1894 \text{ psi/(BPD)/cycle}$ and intercept $b' = 1.5572 \text{ psi/BPD}$ (fig 6). The permeability, k and skin factor, s are calculated from equations 2.23 and 2.24 as follows:

$$k = \frac{162.6\mu B}{m'h} = \frac{(162.6)(1.3)(1)}{(0.1894)(100)} = 11.16 \text{ md}$$

$$s = 1.1513 \left[\frac{1.5572}{0.1894} - \log \left(\frac{11.16}{0.2 * 1 * 0.00001 * 0.25^2} \right) + 3.2275 \right] = 4.027$$

3.2.2 Conventional Method: Semilog Plot

From the semilog plot of $\frac{P_i - P_{wf}(t)}{q_n}$ versus t_{eq} (Fig 7), a straight line drawn for real

time overlaps exactly the t_{eq} straight line .The regression line for t_{eq} -straight line yields a slope, $m' = 0.0823 \ln(10) \text{ psi}/(\text{STB}/D)/\text{cycle}$,

$m' = 0.1895 \text{ psi}/(\text{STB}/D)/\text{cycle}$, intercept $b' = 1.557$.

The permeability and skin factor are calculated as illustrated above:

$$k = \frac{162.6 \mu B}{m'h} = \frac{(162.6)(1.3)(1)}{(0.1895)(100)} = 11.15 \text{ md}$$

$$s = 1.1513 \left[\frac{1.5572}{0.1895} - \log \left(\frac{11.15}{0.2 * 1 * 0.00001 * 0.25^2} \right) + 3.2275 \right] = 4.023$$

3.2.3 Tiab's Direct Synthesis

Data for Tiab's Direct Synthesis are also included in Table 3.3, Fig. 9 shows a log-log plot of $\Delta P/q$, psi/STB and $t^*(\Delta P/q)'$, psi/STB versus t , hrs on the same graph. The infinite acting line can be clearly depicted, and the following values are read from the graph(fig 9) as follows:

$$(t^*(\Delta P/q)')_r = 0.082 \text{ psi/BPD}$$

$$(\Delta P/q)_r = 1.820 \text{ psi/BPD}$$

$$t_r = 19 \text{ hrs}$$

The permeability and skin factor are obtained using equations 2.40 and 2.42 respectively as

$$\text{Permeability}, k = \left(\frac{70.6 \mu B}{h(t_x \Delta P'_q)_r} \right) = \left(\frac{70.6 * 1 * 1.3}{100 * 0.082} \right) = 11.19 \text{ md}$$

$$\text{SkinFactor}, s = 0.5 \left[\left(\frac{1.820}{0.082} \right) - \ln \left(\frac{11.9 * 19}{0.2 * 1 * 0.00001 * 0.25^2} \right) + 7.43 \right] = 4.19$$

3.3 Three Rate Test

3.3.1 Pressure Function for Three-Rate Test.

The three rate test is a particular case of the multirate test and can be evaluated as follows:

$$\frac{P_i - P_{wf}(t)}{q_N} = m_3 X_3 + b_3 \quad (3.3.1)$$

$$\text{where } X_3 = q_2 \left[\log \left(\frac{\Delta t_1 + \Delta t_2}{\Delta t_2} \right) + \frac{q_1}{q_2} \log \left(\frac{t_1 + \Delta t_1 + \Delta t_2}{\Delta t_1 + \Delta t_2} \right) + \frac{q_3}{q_2} \log \Delta t_2 \right] + b_3 \quad (3.3.2)$$

Note that the rate corresponding to each plotted pressure point is q_N -the last rate that can affect that pressure. Earlougher illustrated that a Cartesian plot of $\frac{P_i - P_{wf}(t)}{q_N}$ versus X_3 is a straight line of slope m_3 .

$$m_3 = \frac{162.6 \mu B}{Kh} \quad (3.3.3)$$

$$\text{and intercept } b_3 = m_3 \left[\log \left(\frac{k}{\Phi \mu C_t r_w^2} \right) - 3.2275 + 0.8659S \right] \quad (3.3.4)$$

The formation permeability, k is obtained from equation (3.3.3) and skin, s from (3.3.4)

3.3.2 Pressure Derivative for Three-Rate Test

For this case a derivative with respect to equation (3.3.1) yields:

$$\frac{d}{dt}[\Delta P] = m_3' q_2 \left[\frac{q_3}{q_2} \frac{1}{\Delta t_2} - \frac{q_1}{q_2} \frac{t_1}{[(\Delta t_1 + \Delta t_2)(t_1 + \Delta t_1 + \Delta t_2)]} - \frac{\Delta t_1}{\Delta t_2 (\Delta t_1 + \Delta t_2)} \right] = m_3' X_3' \quad (3.3.5)$$

A plot of $\frac{d}{dt}[\Delta P]$ versus X_3' on a Cartesian graph is a straight line of zero intercept having a slope m_3' as shown in equation (3.3.6)

$$m_3' = \frac{70.6 \mu B}{kh} \quad (3.3.6)$$

The formation Permeability, k is obtained using equation (3.3.6)

3.3.3 Numerical Example For Three-Rate Test

The set of pressure-time data for multirate test (Table 3.1.1 and 3.1.2) is used, only this time the first three flow rates and the corresponding pressure-time data are considered.

3.3.3.1 Pressure-Function

Fig. 10 shows the Cartesian plot of $\Delta P/q$, psi/BPD versus F_{P3} . From the straight line, slope $m_3 = 1.113$ psi/(stb/d cycle), and the intercept $b_3 = 2.0470$ psi/(stb/d).

The formation permeability is computed from Eq. 2.14 as

$$k = \frac{162.6 \mu B}{m'h} = \frac{(162.6)(4.2)(1.12)}{(1.0525)(38)} = 18.08 \text{ md}$$

3.3.3.2 Pressure Derivatives

Fig. 11 is a Cartesian plot of $\Delta P'$, psi/hr versus Σ , BPD/hr. The straight-line of best fit of this graph indicates a slope $m'' = 0.489$ and the new permeability is calculated as follows using eqn. 2.26 :

$$m'' = \frac{70.6\mu B}{kh}$$

$$k = \frac{70.6\mu B}{m''h} = \frac{(70.6)(4.2)(1.12)}{(0.489)(38)} = 17.87\text{md}$$

3.4 Two Rate Test

A two rate test is a special case of generalized multirate test which can be used to determine all the parameters that can be obtained from a pressure buildup test. Consider a well which was flowing at a constant rate q_1 for a period t_1 before its rate was changed to q_2 (Fig. 2). In this case, the bottom hole pressure response after the rate change is given as:

$$P_i - P_{wf} = \frac{141.2\mu B}{kh} \left(q_1 P_D \left[1, (t_1 + \Delta t)_D \right] + (q_2 - q_1) P_D (1, \Delta t_D) + q_2 S \right) \quad (3.4.1)$$

where time after rate changes $\Delta t = t - t_1$

Immediately after the rate change, the second dimensionless pressure in the right hand side of eqn 3.1.1 may be replaced by the logarithmic approximation to obtain

$$P_i - P_{wf} = \frac{141.2\mu B}{kh} \left(q_1 P_D \left[1, (t_1 + \Delta t)_D \right] + (q_2 - q_1) \left[\frac{1}{2} (\ln \Delta t_D + 0.80907) \right] + q_2 S \right) \quad (3.4.2)$$

Adding and subtracting $0.5 \ln(t_1 + \Delta t)_D$ to the right hand side gives:

$$\begin{aligned} P_{wf} = & \frac{-162.6q_1\mu B}{kh} \left[\log \left(\frac{t_1 + \Delta t}{\Delta t} \right) + \frac{q_2}{q_1} \log \Delta t \right] \\ & + P_i - \frac{162.6q_1\mu B}{kh} \left[\frac{P_D \left[1, (t_1 + \Delta t)_D \right] - 0.5 \left[\ln(t_1 + \Delta t)_D + 0.80907 \right]}{1.1513} \right] \\ & - \frac{162.6q_1\mu B}{kh} \frac{q_2}{q_1} \left[\log \left(\frac{k}{\Phi \mu C_t r_w^2} \right) - 3.23 + 0.87s \right] \end{aligned} \quad (3.4.3)$$

If t_1 is so small such that $(t_1 + \Delta t)$ is in the early transient flow period, then the dimensionless pressure in equation (3.4.3) may be replaced by its log approximation and the equation simplifies to:

$$P_{wf} = -\frac{162.6q_1\mu B}{kh} \left[\log \left(\frac{t_1 + \Delta t}{\Delta t} \right) + \frac{q_2}{q_1} \log \Delta t \right] + P_i - \frac{162.6q_1\mu B}{kh} \frac{q_2}{q_1} \left[\log \left(\frac{k}{\Phi\mu C_t r_w^2} \right) - 3.23 + 0.87s \right] \quad (3.4.4)$$

Moreover except for those data affected by early time phenomena such as wellbore storage and skin effect, all pressure data will lie on the straight line. Formation permeability, k is obtained from eqn (3.4.5) while the initial reservoir pressure is obtained from eqn (3.4.6) after first determining the total skin factor, s .

If t_1 is large such that $(t_1 + \Delta t)$ is no longer in the early transient flow period. Then eqn (3.4.3) may be written for small values of Δt in which $\Delta t \ll t_1$ as follows:

$$P_{wf} = -\frac{162.6q_1\mu B}{kh} \left[\log \left(\frac{t_1 + \Delta t}{\Delta t} \right) + \frac{q_2}{q_1} \log \Delta t \right] + P_i - \frac{162.6q_1\mu B}{kh} \left[\frac{P_D(1, t_{1D}) - 0.5 [\ln t_{1D} + 0.80907]}{1.1513} - \frac{162.6q_1\mu B}{kh} \frac{q_2}{q_1} \left[\log \left(\frac{k}{\Phi\mu C_t r_w^2} \right) - 3.23 + 0.87s \right] \right] \quad (3.4.5)$$

equation (3.4.4) & (3.4.7) is same as:

$$P_{wf} = -\frac{162.6q_1\mu B}{kh} \left[\log \left(\frac{t_1 + \Delta t}{\Delta t} \right) + \frac{q_2}{q_1} \log \Delta t \right] + P - \frac{162.6q_1\mu B}{kh} \frac{q_2}{q_1} \left[\log \left(\frac{k}{\Phi\mu C_t r_w^2} \right) - 3.23 + 0.87s \right] \quad (3.4.6)$$

where P^* is extrapolated pressure which was encountered in Horner's pressure buildup equation.

3.4.1 Pressure Function For A Two Rate Test

For a two rate test, it is observed that the pressure behaviour caused by variable flowrate from equation (3.4.6) is given by:

$$P_{wf} = m_2 \left[\log \left(\frac{t_1 + \Delta t}{\Delta t} \right) + \frac{q_2}{q_1} \log \Delta t \right] = m_2 X_2 + P_{int} \quad (3.4.7)$$

$$\text{where time corresponding to the first flowrate } t_1 = \frac{24N_P}{q_1} \quad (3.4.8)$$

A plot of P_{wf} versus $\left[\log \left(\frac{t_1 + \Delta t}{\Delta t} \right) + \frac{q_2}{q_1} \log \Delta t \right]$ will be linear with slope m_2 and pressure intercept P_{int} which are given as:

$$m_2 = \frac{-162.6q_1\mu B}{Kh} \quad (3.4.9)$$

$$P_{int} = P_i - m_2 \left[\log \left(\frac{k}{\Phi \mu C_t r_w^2} \right) - 3.2275 + 0.87S \right] \quad (3.4.10)$$

Pinson showed that for $t_1 \gg \Delta t$, then $\log(t_1 + \Delta t) \approx \log \Delta t$ and the plotting function may be simplified by rearranging equation (3.4.7) as follows:

$$P_{wf} = m_2'' [\log \Delta t + P_{int}] \quad (3.4.11)$$

A plot of the P_{wf} versus Δt is a straight line of slope m_2' and intercept given as:

$$m_2'' = \frac{-162.6(q_2 - q_1)\mu B}{kh} \quad (3.4.12)$$

$$P_{int} = P_i + \frac{m_2'' q_2}{(q_2 - q_1)} \left[\log \left(\frac{k}{\Phi \mu C_t r_w^2} \right) - 3.2275 + 0.87S \right] + \frac{q_2}{q_1} \log \Delta t \quad (3.4.13)$$

where $P_i \equiv$ false pressure (P^*) which is obtained from the intercept P_{int} using equation (3.4.13)

$$P^* = P_{int} - \frac{q_2}{(q_1 - q_2)} [P_{wf}(\Delta t = 0) - P_{1hr}] \quad (3.4.14)$$

The false pressure (P^*) obtained can be corrected to the current average pressure using the MDH dimensionless pressure function as highlighted below:

$$\text{Average Pressure, } \bar{P} = P - m_2 \left(\frac{P_{DMBH}}{2.303} \right) \quad (3.4.15)$$

$$\text{where } P_{DMBH} = 2.3 \log t_{PDA} + 3.5 \quad (3.4.16)$$

$$t_{PDA} = \frac{0.0002637 * K * t_1}{\Phi \mu C_t C_A} \quad (3.4.17)$$

Formation permeability is obtained from eqn(3.4.12) and skin factor from intercept as follows:

$$s = 1.1513 \left[\frac{q_1}{(q_1 - q_2)} \frac{(P_{wf}(\Delta t = 0) - P_{1hr})}{m''} \right] - \log \left(\frac{k}{\Phi \mu C_t r_w^2} \right) + 3.2275 \quad (3.4.18)$$

$$\text{Flow Efficiency, } FE = 1 - \frac{\Delta P_s}{P - P_{wf}(\Delta t = 0)} \quad (3.4.19)$$

3.4.2 Pressure Derivative For Two Rate Test

For this test, the derivative of eqn(3.4.7) with respect to time is

$$P_{wf}' = m_2' \frac{1}{\Delta t} \left[\frac{q_2}{q_1} - \frac{t_1}{t_1 + \Delta t} \right] = m_2' X' \quad (3.4.20)$$

A Cartesian plot of P_{wf}' versus X' will yield a straight line of slope m_2'

$$m_2' = \frac{70.6 q_1 \mu B}{Kh} \quad (3.4.21)$$

3.4.3 Tiab's Direct Synthesis For Two Rate Test

In 1993, Tiab introduced a new technique that used log-log plots of the pressure and pressure derivatives to obtain characteristic points of intersection of various straight line portions of these straight lines.

This technique termed TDS is also applicable to two, three and multirate test. Assuming the infinite acting line is observed, the formation permeability and skin can be calculated from the relations:

$$k = \frac{162.6 (q_2 - q_1) \mu B}{h (t^* \Delta P')_r} \quad (3.4.22)$$

$$s = 0.5 \left[\frac{(\Delta P)_r}{(t^* \Delta P')_r} - \ln \left(\frac{kt_r}{\Phi \mu C_t r_w^2} \right) + 7.43 \right] \quad (3.4.23)$$

where ΔP_r and $(t^* \Delta P')_r$ are values of ΔP and $t^* \Delta P'$ corresponding to any time during the infinite acting radial flow time. The derivative of pressure in equation(3.4.6) with respect to time yields:

$$(t^* \Delta P') = \frac{70.6 (q_2 - q_1) \mu B}{kh} \quad (3.3.24)$$

Its obvious from equation (3.4.21) that $(t^* \Delta P')$ is a constant value as long as the radial flow regime (corresponding to the infinite acting behaviour) is dominant.

3.4.4 Numerical Example for a Two-Rate Test.

A two rate flow test was conducted in a medium permeability sandstone reservoir. In preparation for the test, the well was stabilized at a rate of 107 STB/D on a 12/64 inch choke. The rate was reduced to 46 STB/D by reducing the choke size to 7/64 inch. The bottom hole pressure were measured for a period starting from 4 hrs before the rate changed to 22hrs after the rate change. The measured pressure data is

tabulated in fig. 3.2. Estimated rock and fluid properties are as follows:

RESERVOIR PARAMETERS					
Porosity, Φ	0.12		q1	107.0	STB
Oil FVF, B_o	1.5	RB/STB	q2	46.0	STB
Height, h	13	ft	Np	26400	STB
Compressibility, C_t	0.0000120	psi ⁻¹			
Wellbore Radius, r_w	0.276	ft			
Oil Viscosity, μ	0.6	cp			
Eff. Wellbore Radius, r_e	∞				

where

$$X = \left[\log \frac{t_1 + dt}{dt} + \frac{q_2}{q_1} \log dt \right] \quad \text{and} \quad X' = \frac{1}{dt} \left[\frac{q_2}{q_1} - \frac{t_1}{t_1 + dt} \right]$$

3.4.4.1 Pressure Function for the Numerical Example

Fig. 12 is a Cartesian plot of P_{wf} versus X where the time corresponding to the first flow rate t_1 was calculated from equation(3.4.8) as $t_1 = 5921.5$ hrs.

From the graph , the slope $m_2 = -95.33$ & intercept $P_{int} = 3526.44$ psi.

The formation permeability k , is obtained using equation (3.4.9) as follows:

$$k = \frac{-162.6 q_1 \mu B}{m_2 h} = \frac{-162.6 * 107 * 1.5 * 0.6}{-95.33 * 13} = 12.63 \text{ md}$$

The value of P_{wf} (at 1hr) @ $X = 3.77$ is read directly from straight line in fig. 12 as

$P_{1hr} = 3168.5$ psi, and P_{wf} @ $\Delta t = 0$ is 2857 psi.

Thus the skin factor, s is estimated from equation (3.4.15) as

$$s = 1.1513 \left[\frac{107}{(107 - 46)} \left(\frac{2857 - 3168.5}{-95.33} \right) \right] - \log \left(\frac{12.63}{0.12 * 0.6 * 12 * 10^{-6} * 0.276^2} \right) + 3.2275 = 0.8$$

3.4.4.2 Pressure Derivative for the Numerical Example

A Cartesian plot of $\Delta P'$ versus X' yields slope $m_2' = 41.85$ psi (fig. 13). and formation permeability k is obtained from equation (3.4.21) as follows:

$$k = \frac{70.6 q_1 \mu B}{m_2' h} = \frac{70.6 * 107 * 1.5 * 0.6}{41.85 * 13} = 12.50 \text{ md}$$

3.4.4.3 Tiab's Direct Synthesis.

Figure 14 shows a log-log plot of ΔP & $t^* \Delta P'$ versus time, t . Note that in this case $t_i = 5923$ hrs is significantly large and consequently the infinite acting line can be clearly defined.

From fig. 13 the infinite acting line indicates a value $t^* \Delta P' = 23 \text{ psi} - \text{hr}$.

Formation permeability, k is obtained from equation (3.4.24) as:

$$k = \frac{70.6 (q_2 - q_1) \mu B}{(t^* \Delta P') h} = \frac{70.6 * (107 - 46) * 0.6 * 1.5}{23 * 13} = 12.96 \text{ md}$$

Thus the skin corresponding to a value of $(\Delta P)_r = 360$ psi and $(t^* \Delta P')_r = 23$ at $(t)_r = 10$ hrs, is calculated from equation (23) as follows:

where formation permeability as computed above is $k = 12.63$ md

$$s = 0.5 \left[\frac{(\Delta P)_r}{(t^* \Delta P')_r} - \ln \left(\frac{k t_r}{\Phi \mu C_t r_w^2} \right) + 7.43 \right] = 0.5 \left[\frac{360}{23} - \ln \left(\frac{12.63 * 10}{0.12 * 0.6 * 12 * 10^{-6} * 0.276^2} \right) + 7.43 \right] = 0.9$$

All the above test can be performed whether the well is producing in the transient or semi-steady state. In the later case, the test may also provide information for an estimate of the average reservoir pressure as obtain from equation (3.4.14) below:

$$P^* = P_{int} - \frac{q_2}{(q_1 - q_2)} [P_{wf}(\Delta t = 0) - P_{1hr}] = 3526.44 - \frac{46}{(107 - 46)} [2856.0 - 3168.5] = 3762.1 \text{ psi}$$

The P^* obtained may be corrected to the current average reservoir pressure using equations (3.4.15), (3.4.16) and (3.4.17) as shown:

From eqn (3.4.17)

$$t_{PDA} = \frac{0.0002637 * 12.63 * 5922}{0.12 * 0.6 * 12 * 10^{-6} * (40 * 43560)} = 13.102 \text{hrs}$$

From equation (3.4.16), assuming the well is at the centre of a circular reservoir, then

$$P_{DMBH} = 2.3 * \log(13.102) + 3.5 = 6.07$$

substituting equations (3.4.16) and (3.4.17) into (3.4.15) gives:

$$\bar{P} = 3762.1 - 95.33 \left(\frac{6.07}{2.303} \right) = 3510.8 \text{ psi}$$

CHAPTER 4

DATA ANALYSIS, RESULTS, AND DISCUSSIONS

4.1 Introduction

The pressure derivative is applicable for all three types of well tests, multirate, three rate and two rate tests as illustrated with numerical examples in chapter 3. The different techniques used yield results that are in good agreement. Summary of results is listed in tables 4.1 and 4.2. The comparison between actual and calculated data is displayed in figure 8. As shown, the calculated data agree well with the actual well data. The error using real time instead of equivalent time is relatively small because the flowrate is decreasing gradually and has a smoother behaviour. Therefore, it would be better to plot the normalized pressure versus time when the rate is changing slightly to obtain acceptable results.

4.2 Analysis for Multirate Test

The different techniques used yield results that are in good agreement. Summary of results for continuously changing flowrate and constant flowrate is listed in Table 4.1 and 4.2 respectively. The permeability and skin factor estimated by the various methods as observed in table 4.1 shows strong agreement for the various techniques used. The permeability estimated using pressure function for constant flowrate (Table 4.2) gives an underestimation of the permeability. This is because the choice of $m'=1.0525\text{psi/STB}$ as obtained from Figure 3 is incorrect. The value of permeability computed from this slope is 19.12md. The permeability value obtained using a semi-log pressure function is much closer to the permeability value obtained from the pressure derivative method. The pressure derivative method gives a more accurate result than the pressure function. The primary purpose of the derivative is to make sure that the appropriate straight line, for calculating k , is selected properly.

4.3 Analysis for Three Rate Test

For the three rate test, the permeability values obtained using pressure function and pressure derivative techniques are less compared to multirate test. This is because the early data are affected by noise.

4.4 Analysis for Two Rate Test

Table 4.3 gives a summary of results obtained by various techniques for a two rate test. The value obtained by Tiab's Direct Synthesis technique, is in good

agreement with the one obtained from conventional analysis. This shows the importance of designing a well test such that the first flow-rate is long enough, in this case $t_1 = 5923$ hrs, to obtain a well defined infinite-acting line (Fig. 14).

4.5 Summary

The derivative curve using real time, Δt , shows a downward trend. Although the derivative is plotted versus Δt_{eq} , it still bows downward. This is due to the boundary effect. Fig. 9 shows that the last points of the derivative curve lie on a straight line of slope 1. This is an indication that the radius of investigation reached all boundaries during the first flowing period, so that the pseudo-steady state flow was achieved.

The comparison between actual and calculated data is illustrated on Fig. 8. There is an excellent matching for all times. This is due to the fact that the equations used for the computation are for infinite acting radial flow.

CHAPTER 5

SUMMARY, CONCLUSIONS AND RECOMMENDATIONS

5.1 Summary

The objective of this study is to apply pressure derivative concept to multirate test. The above objective was achieved by analysing various types of tests which include multirate test for a continuously changing flowrate and constant flowrate preceded by a variable flowrate, two rate and three rate tests. All results found by using different techniques as listed in Tables 4.1, 4.2 and 4.3. It should be noted that all results are in good agreement. A two-rate test yields the same results as those obtained from a constant rate drawdown test when the 2nd rate is higher than the first rate. The derivative curve using real time, Δt , shows a downward trend. Although the derivative is plotted versus Δt_{eq} , it still bows downward. This is due to the boundary effect. Fig. 9 shows that the last points of the derivative curve lie on a straight line of slope 1. This is an indication that the radius of investigation reached all boundaries during the first flowing period, so that the pseudo-steady state flow was achieved.

5.2 Conclusions

Based on the results obtained from the study, the following conclusions were reached:

1. Multirate tests are a practical alternative to buildup testing. The benefits besides minimizing differed production is that a better reservoir description is obtained from the analysis of the obtained pressure data.
2. The pressure derivative concept is applicable to all three types of well tests, multirate, three rate and two rate tests.
3. Tiab's direct synthesis is extended to multirate tests for oil reservoirs hence type curve matching is no longer required to analyse such a test. This technique is illustrated by several numerical examples and the results obtained are in good agreement with those estimated by other techniques.
4. Tiab's Direct Synthesis is applicable to all multirate tests.
5. Pinson's and Tiab's Direct Synthesis methods should be used only when the time corresponding to the first flowing period t_1 is sufficiently large (i.e. $t \gg \Delta t$). This is required in order to make possible the identification of the infinite acting line behaviour.

6. The conventional pressure derivative technique does not have such a restriction.
7. When flowrate has a smooth variation, the results, found by using real time are excellent, whereas sudden rate changes provide unacceptable results.
8. Data should be recorded at equal time intervals during the whole test, in order to obtain a smooth pressure derivative curve.
9. If the flowrate varies smoothly, the use of the rigorous method (Superposition time) is time consuming since the plot of the normalized pressure versus flowing time yields acceptable results.

5.3 Recommendations

The following areas have been identified for improvement in the application of pressure derivative concept to analysing multirate tests:

1. The use of regression and numerical simulation methods is highly suggested for data analysis.
2. Appropriate surface production testing equipment should be used in multirate test. Choke manifold are extremely important for controlling flow-rates. Maximum versatility in well-flow control and shut-in is a must.

NOMENCLATURE

B	oil volumetric factor, rb/STB
b_{ng} , b'	intercept (multi rate tests)
c	compressibility, 1/psi
C	wellbore storage, bbl/psi
C_D	dimensionless storage constant
D	turbulence factor
h	formation thickness, ft
k	formation permeability, md
N,n	number of flow periods (rates)
m'	slope (multi rate tests)
m_{ng}	slope (multi rate tests)
m''	slope from the pressure derivative plot
$m(P)$	pseudo-pressure function
P	pressure, psi
P'	pressure derivative, psi/hr
P_{wf}	well flowing well pressure, psi
P_D	dimensionless pressure
P_i	Initial pressure, psi
q	oil flow rate, BPD
q_{ref}	any fixed reference surface rate
r_w	Wellbore radius, ft
r	radius, ft (distance between observation and active well)
r_D	dimensionless radius
r_s	skin radius, ft
s	mechanical skin factor
S_a	apparent skin factor
t	test time, hr
t_D	dimensionless time calculated using the radius
t_{eq}	equivalent flow time, hr
t_{Deq}	equivalent dimensionless flow time
T_r	transmissibility = kh/μ , md-ft/cp; reservoir temperature, ° R
X_n	superposition time, defined by eq. 3.2

GREEK SYMBOLS

Δ	change, drop
ΔP	pressure difference, psi
ΔP_D	dimensionless pressure change or response amplitude
$\Delta P'$	change of rate of pressure with time (pressure derivative), psi
ΔP_q	defined by Eq. 2.28.2, psi/STB or psi/SCF
$\Delta P'_q$	derivative of ΔP_q with respect to time
Δt	flow time, hr
Δt_{Deq}	equivalent dimensionless flow time
Σ	parameter defined by Eq. 3.1
Φ	porosity
μ	viscosity, cp

SUBSCRIPTS

avg	average
D	Dimensionless quantity
f	formation, or intrinsic fracture property
i	Initial conditions, image/imaginary
L	linear
o	oil
R,r	radial flow; rock; real
sc	standard conditions
t	total
w	wellbore; water
wf	Flowing conditions

REFERENCES

1. Russell, D.G. *Determination of Formation Characteristics From Two-Rate Flow Tests*. JPT (Dec. 1963), p. 1374-1355; Trans., AIME, **228**.
2. Selim, M.A. *A Modification of the Two-Rate Flow Method For Determination of Reservoir Parameters*. J. Institute of Petroleum (Nov.1967) 53, N°527
3. Pinson A. E. Jr. *Conveniences in Analyzing Two-Rate Flow Tests*. JPT (Sept.1972), p. 1139-1141.
4. Earlougher, R. C., Jr. *Estimating Errors When Analyzing Two-Rate Flow Tests*. JPT (May 1973), p. 545-547.
5. Odeh, A.S., Jones, L.G. *Two-Rate Flow Test, Variable Rate Case*. JPT (Jan. 1974), p. 93-99; *Trans. AIME*, **257**.
6. Doyle, R. E. and Sayegh, E. F. *Real Gas Transient Analysis of Three-Rate Flow Tests*. JPT (Nov. 1970), p. 1347-1356; Paper SPE 2607 presented At SPE 44th Annual Fall Meeting, Denver, CO. 1969.
7. Tiab, D. *Analysis of Pressure and Pressure Derivatives Without Type-Curve Matching: 1-Skin and Wellbore Storage*. SPE 25426 Production Operations Symposium, Oklahoma (Mar. 1993), p. 203-216.
8. Tiab, D. *Direct Type–Curve Synthesis of Pressure Transient Tests*. Paper SPE 18992 presented at SPE Joint Rocky Mountain Regional/Low Permeability Reservoirs Symposium and Exhibition, Denver, CO, March 6-8, 1989.
9. Tiab, D. *Analysis of Pressure and Pressure Derivatives Without Type -Curve Matching: 2- Vertically Fractured Wells in Closed Systems*. Journal of Petroleum Science and Eng. Vol.11, (1994), p. 323-333.
10. Amiar, M. *Application of Tiab's Direct Synthesis Technique to Multi-Rate Tests*. MS Thesis. The University of Oklahoma, 1999.
11. Amiar, M. and Tiab, D. *Application of Tiab's Direct Synthesis Technique to Multi-Rate Tests*. Paper SPE 62607 prepared for presentation at the 2000 SPE/AAPG Western Regional Meeting held in Long Beach, California, 19–23 June 2000.
11. Earlougher, R.C., Jr., *Advances in Well Test Analysis*", Monograph Series Vol. 5, SPE, Dallas, TX, 1977.
12. Duhamel, J. M. C. *Mémoire Sur la Methode Générale Relative au*

- Mouvement de la Chaleur Dans les Corps Solides Plongés Dans les Milieux Dont la Temperature Varie Avec le Temps*. J. Ec. Polyt. (Paris) **14** (1833), p. 20-77.
13. Collins, R. E. *Flow of Fluids Through Porous Materials*. Reinhold Publishing Corp., New York (1961), p. 108-123.
 14. Agarwal, R. G. *A New Method to Account for Producing Time Effects When Drawdown Type Curves are Used to Analyze Pressure Buildup and Other Test Data*. Paper SPE 9289 presented at SPE 55th Annual Fall Meeting, Dallas, Texas, Sept. 21-24, 1980.
 15. Van Everdingen, A. F. and Hurst, W. *The Application of the Laplace Transformation to Flow Problems in Reservoirs*. Trans., AIME (1949) 186, p. 305-324.
 16. Agarwal, R. G., Al-Hussainy, R., and Ramey, H. J., Jr. *An Investigation of Wellbore Storage and Skin Effect in Unsteady Liquid Flow: I. Analytical Treatment*", SPEJ (Sept. 1970) 279-290; Trans., AIME, 249.
 17. Wattenbarger, R. A. and Ramey, H. J., Jr. *An Investigation of Wellbore Storage and Skin Effect in Unsteady Liquid Flow: II. Finite Difference Treatment*. SPEJ (Sept. 1970) p. 291-297; Trans., AIME, 249.
 18. Ramey, H. J., Jr. *Short-Time Well Test Data Interpretation in the Presence of Skin Effect and Wellbore Storage*. JPT (Jan. 1970), p. 97-104; Trans., AIME, 249.
 19. Raghavan, R. *Well Test Analysis*. PTR Prentice-Hall, Inc. New Jersey. P. 209-211 (1993).
 20. Lee, J. *Well Test Analysis*. SPE Text Book Series Vol. 1, New York 1982.
 21. Stegemeier, G. L. and Matthews, C. S. *A Study of Anomalous Pressure Buildup Behavior*. Trans., AIME (1958) 213, p. 44-50.
 22. Odeh, A. S. and Jones, L. G. *Pressure Drawdown Analysis, Variable Rate Case*. JPT (Aug. 1965), p. 960-964.
 23. Horne, R. N., and Kuchuk, F. *The Use of Simultaneous Flow Rate and Pressure Measurements to Replace Isochronal Gas Well Tests*. SPE Formation Evaluation, 1988, p. 467-470.
 24. Al Hussainy, R. *Transient Flow of Ideal and Real Gases Through Porous Media*, Ph.D dissertation, Texas A&M U., College Station (May, 1967).

25. Jokhio, S. A. *Interpretation of Deliverability and Pressure Tests in Carbon Dioxide Reservoirs*. M.S Thesis, University of Oklahoma, 1997.
26. Quillian, R. G. *Annotation of Normalization Methods Applied to Variable-Rate Drawdown. Tests From Low-Permeability, Low-Pressure Gas Reservoirs*. Paper CIM 78-29-14, Presented at 29th Annual Technical Meeting of the Petroleum Society of CIM, Calgary, Alberta, June 13-16, 1978.
27. Smith, R.V. *Practical Natural Gas Engineering*. Second Edition, Penn Well Publishing Company, Tulsa, Ok (1990) 162-174.
29. Dominique Bourdet . *Well Test Analysis: The Use Of Advanced Interpretation Models* 1983a page 36-46
- 30 Brian F. Towler, *Fundamental principles of Reservoir Engineering*. Page 65 – 68.
31. *Advanced Calculus (Schaum's Outlines)*, 2nd edition - R. Wriede, S. Spiegel (2002)
32. *Advanced Calculus of Real-Valued functions of a Real Variable & Vector-Valued Function of a Vector Variable* – Hans Sagan, North Carolina State University, Page 141 – 150
33. Roland N. Horne, *Modern Well Test Analysis, A computer Aided Approach*, 2nd edition, Page 65 – 83.
34. Ekwere J. Peters, *Advanced Petrophysics*, page 3.19 – 3.36

APPENDIX A

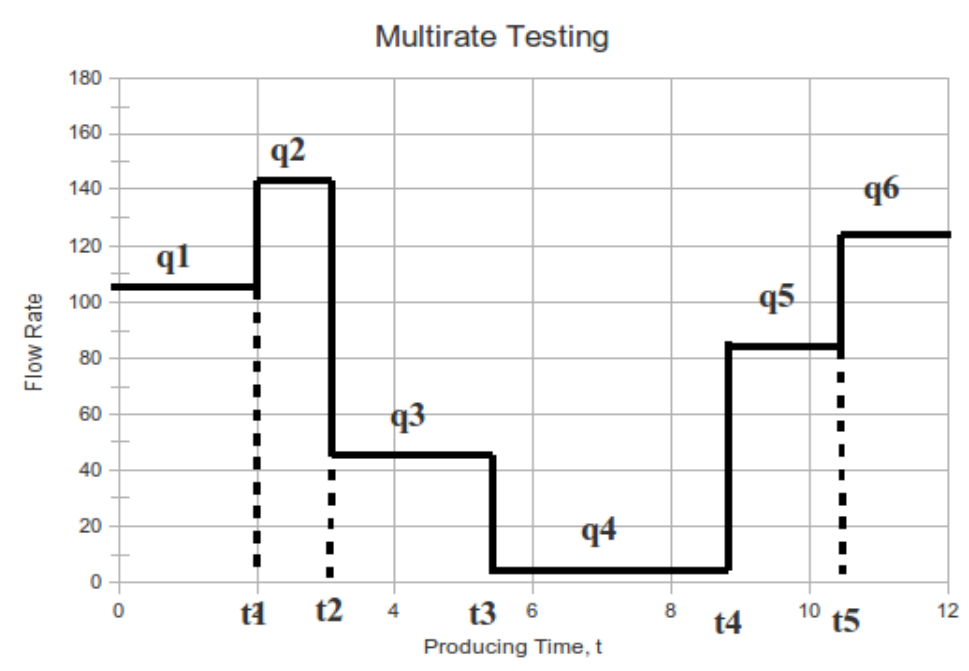


Fig. 1 Schematic representation of a variable production-rate (after Earlougher)

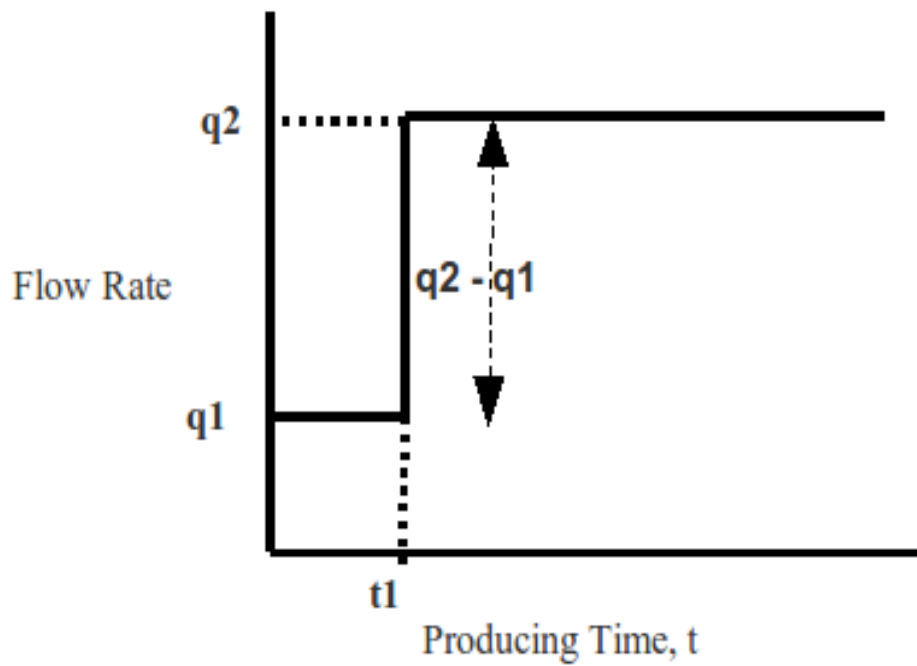


Fig. 2 Schematic representation of a two-rate Test.

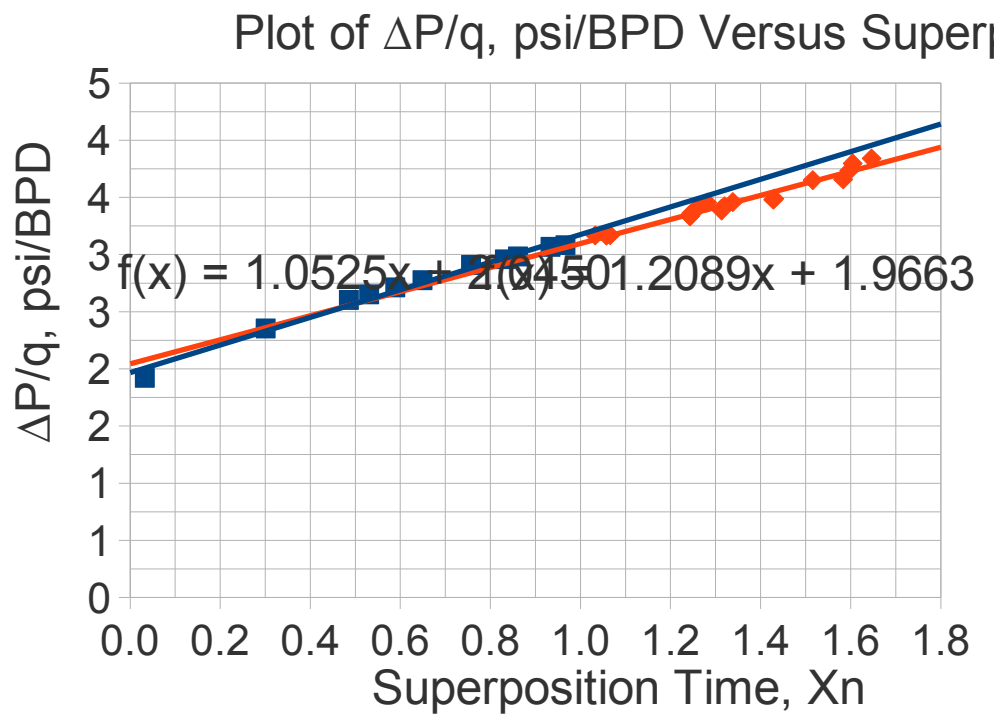


Fig 3. Pressure-Function for the Multi-Rate Test

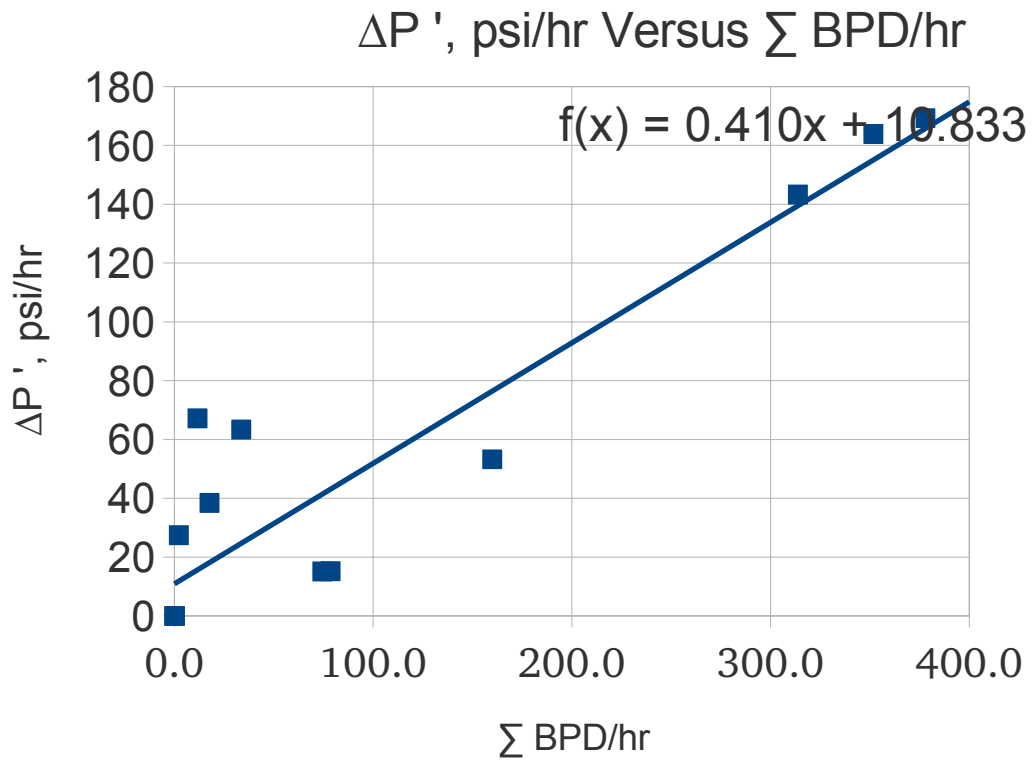


Fig. 4 Pressure-Derivative for the Multi-Rate Test

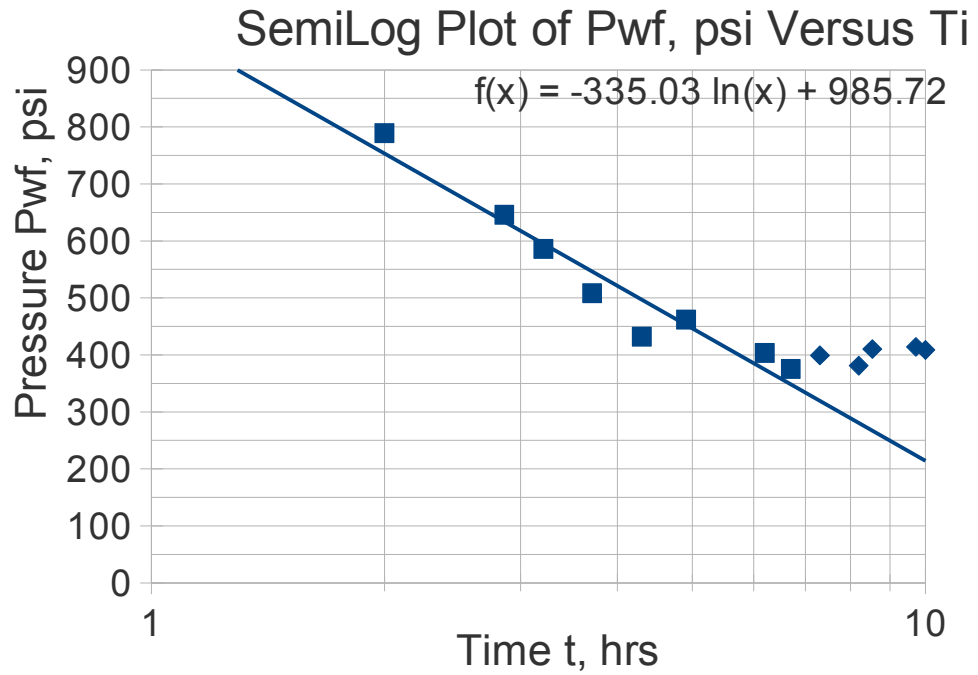


Fig. 5 Semi-Log plot of P_{wf} versus t for the Multi-Rate Test

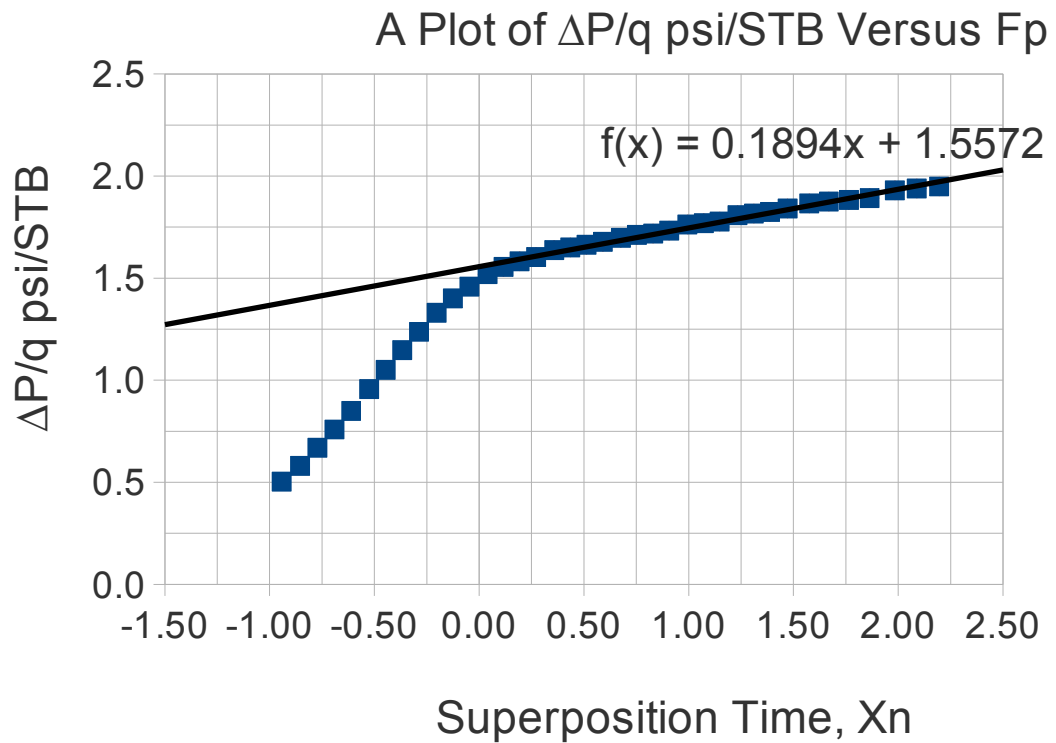


Fig. 6 Cartesian Plot of Normalized Pressure Versus Superposition Time, X_n

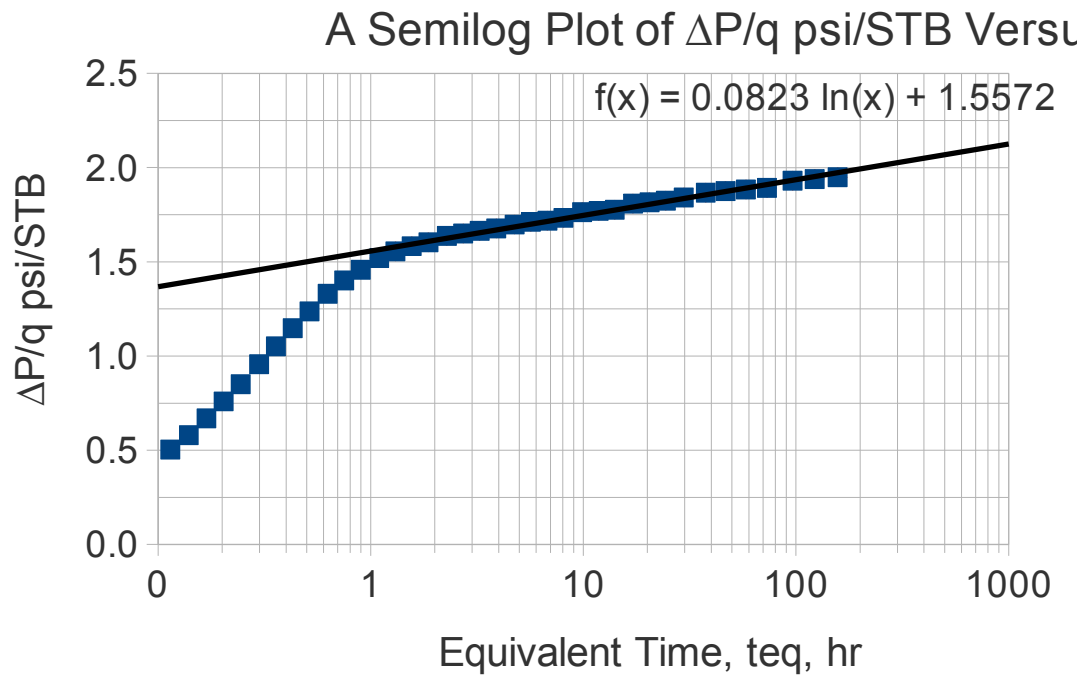


Fig. 7 Semilog Plot of Normalized Pressure Versus Equivalent Time, t_{eq}

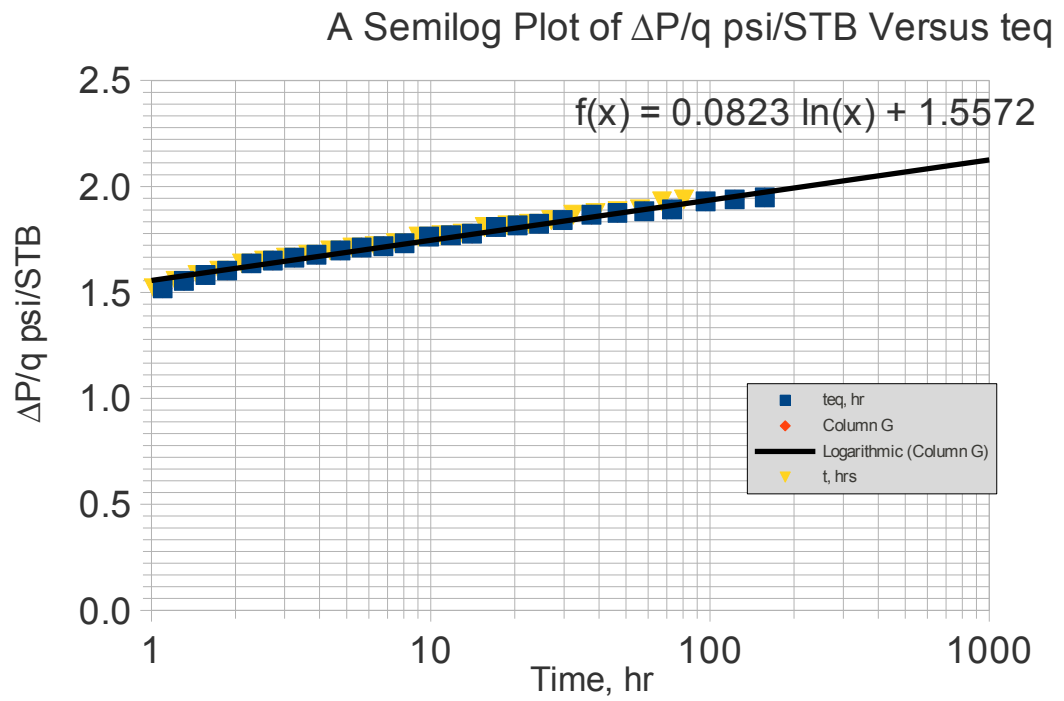


Fig. 8 Semilog Plot of Normalized Pressure Versus Time, t and Equivalent Time, t_{eq}

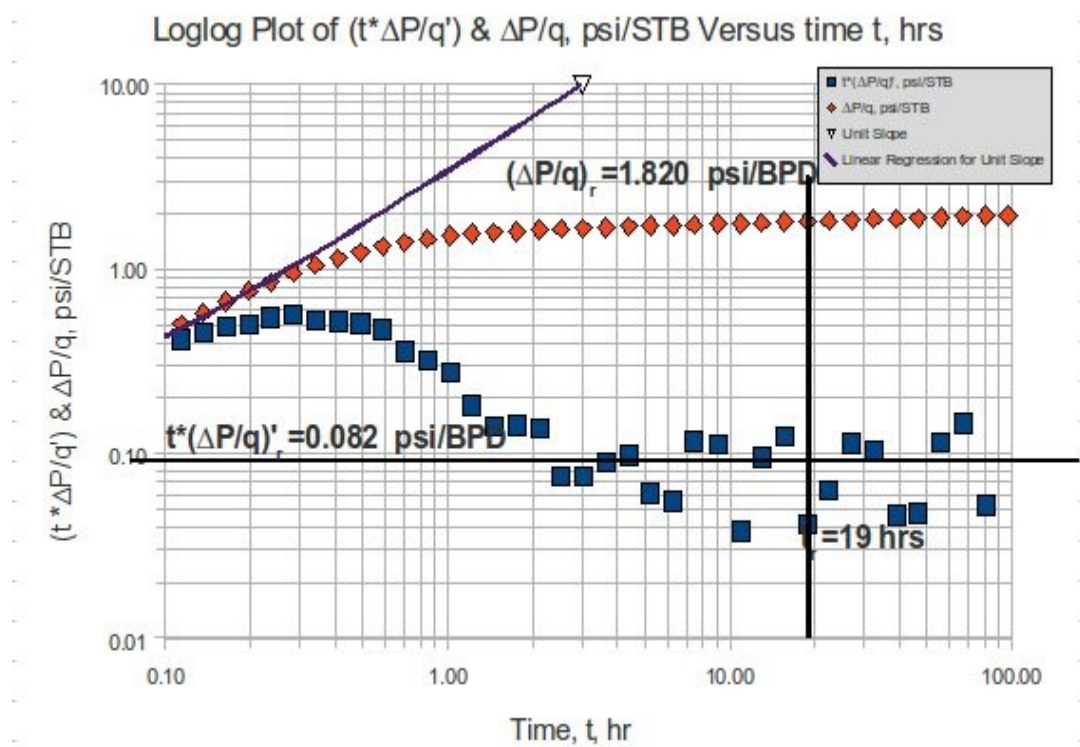


Fig. 9 Loglog Plot of Normalized Pressure and Pressure Derivative Versus Producing Time, t .

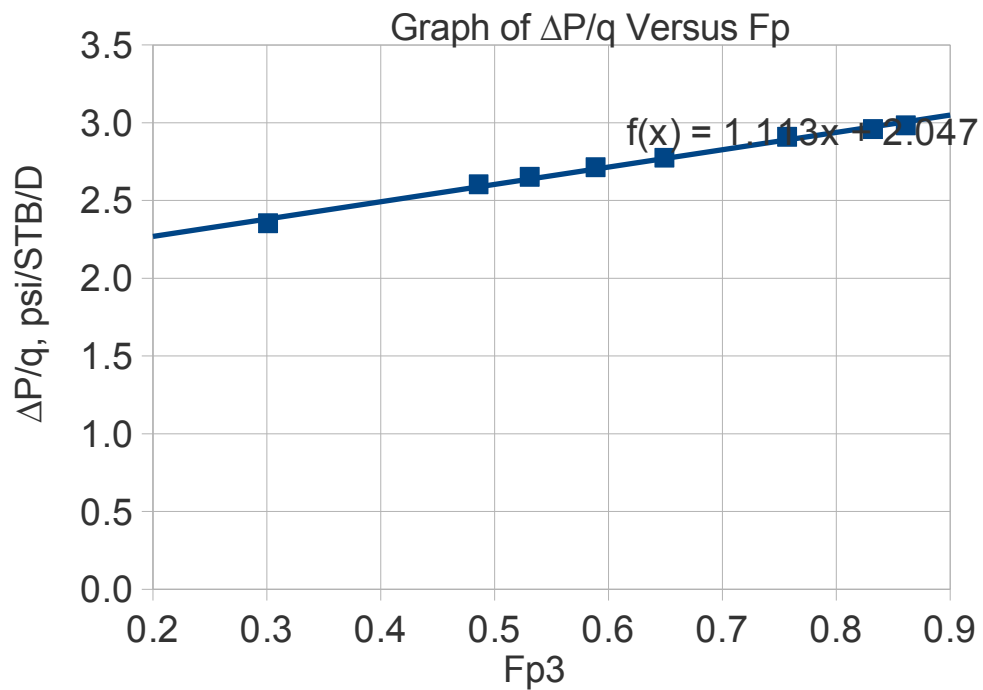


Fig. 10 Pressure-Function for the Three-Rate Test

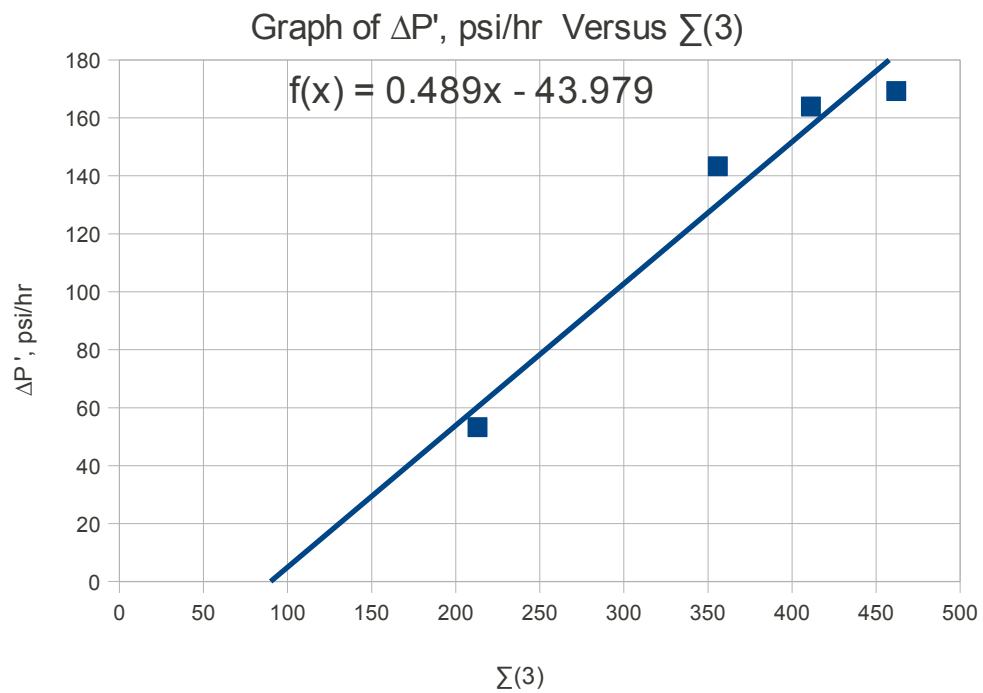


Fig. 11 Pressure-Derivative for the Three-Rate Test

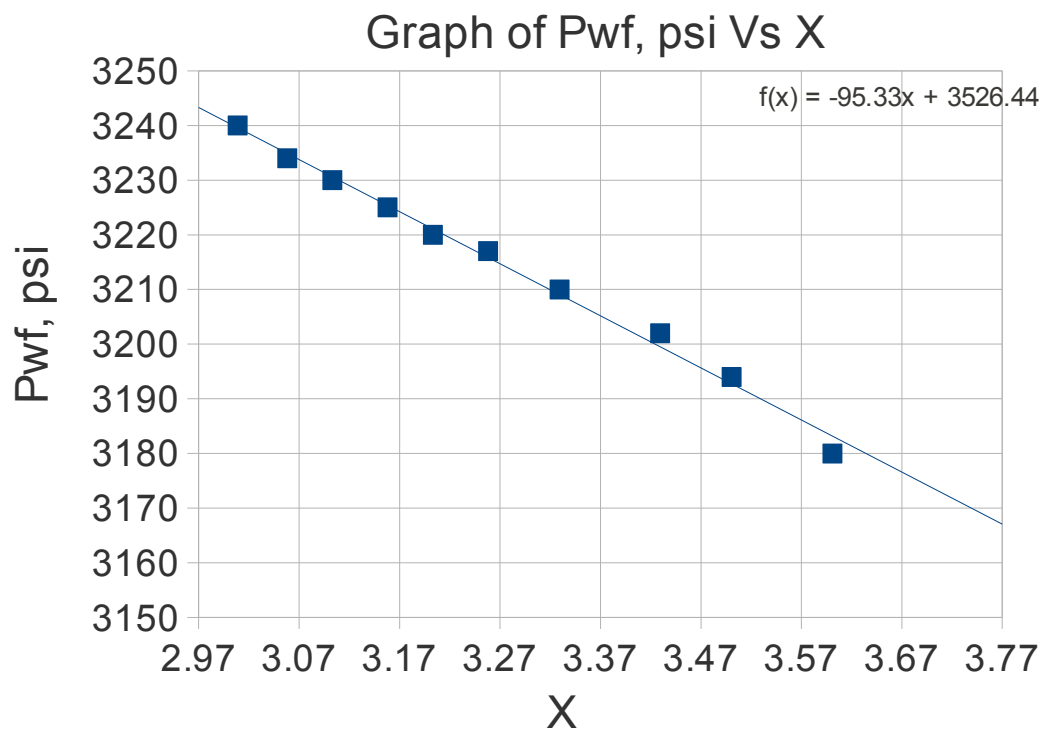


Fig. 12 Pressure-Function for the Two-Rate Test

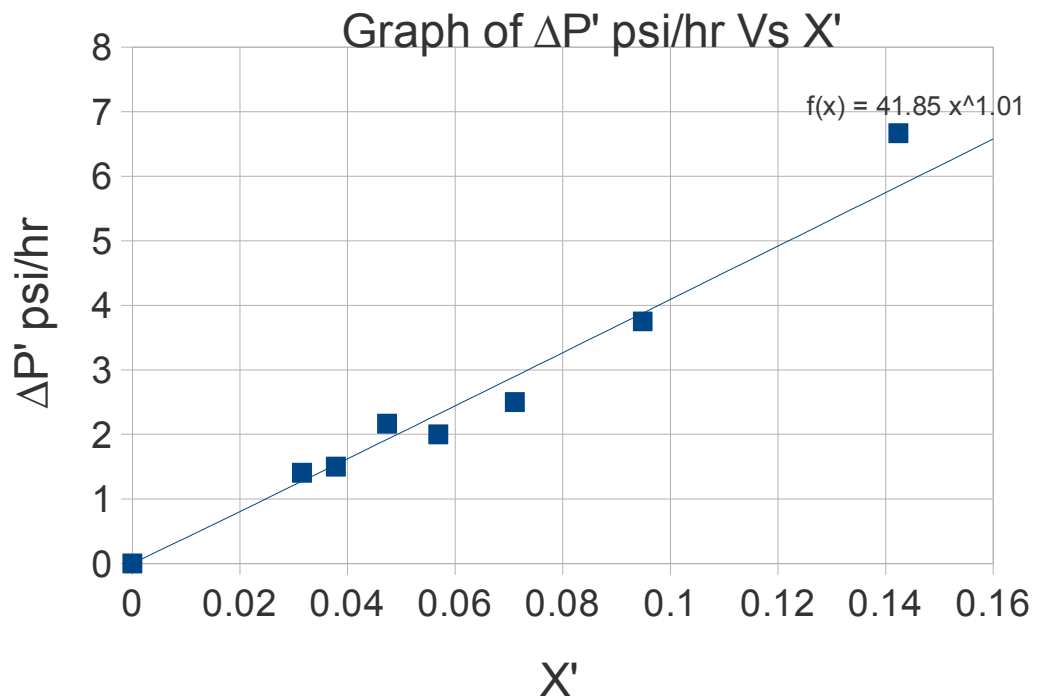


Fig. 13 Pressure-Derivative for the Two-Rate Test

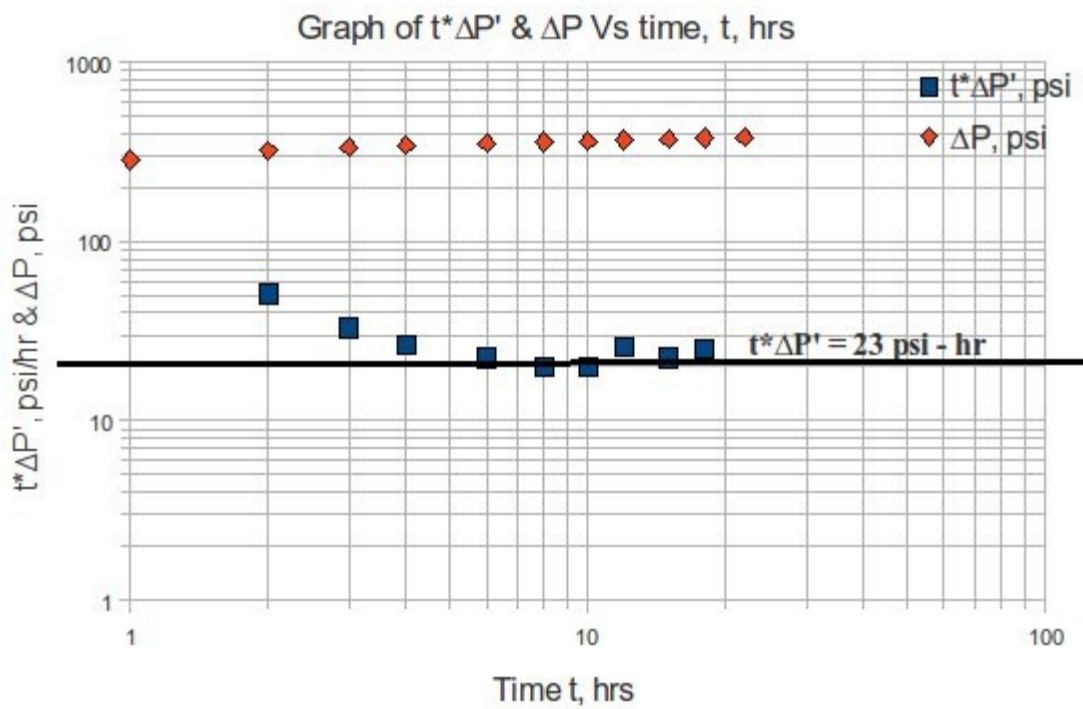


Fig. 14 Direct Synthesis for the Two-Rate Test

APPENDIX B

LIST OF TABLES

BOTTOM HOLE FLOWING PRESSURE DATA							
n	Time, t hrs	pwf, psi	N	q, BPD	ΔP, psi	ΔP/q, psi/BPD	Xn
1	0.0000	3895.12		0	0.00		
2	0.1078	3345.78	1	1320	549.34	0.42	
3	1.0784	1359.82	1	1320	2535.30	1.92	0.0328
4	2.0000	788.98	1	1320	3106.14	2.35	0.3010
5	2.8566	645.96	2	1248	3249.16	2.60	0.4860
6	3.2100	585.80	2	1248	3309.32	2.65	0.5310
7	3.7091	508.50	2	1248	3386.62	2.71	0.5887
8	4.3000	431.98	2	1248	3463.14	2.77	0.6491
9	4.9064	461.96	3	1180	3433.16	2.91	0.7570
10	6.1990	403.52	3	1180	3491.60	2.96	0.8323
11	6.7000	375.28	3	1180	3519.84	2.98	0.8612
12	7.3064	399.06	4	1140	3496.06	3.07	0.9334
13	8.2002	381.06	4	1140	3514.06	3.08	0.9666
14	8.5410	410.24	5	1100	3484.88	3.17	1.0330
15	9.7232	414.04	5	1100	3481.08	3.16	1.0578
16	10.0000	408.68	5	1100	3486.44	3.17	1.0660
17	10.4293	560.88	6	965	3334.24	3.46	1.2815
18	10.7634	613.08	6	965	3282.04	3.40	1.2584
19	11.2100	650.86	6	965	3244.26	3.36	1.2461
20	11.7091	670.64	6	965	3224.48	3.34	1.2425
21	12.1000	677.62	6	965	3217.50	3.33	1.2434
22	12.2918	709.94	7	921	3185.18	3.46	1.3383
23	12.6405	741.82	7	921	3153.30	3.42	1.3200
24	13.0611	762.24	7	921	3132.88	3.40	1.3131
25	13.9900	777.02	7	921	3118.10	3.39	1.3132
26	14.1258	817.34	8	843	3077.78	3.65	1.5158
27	15.8890	953.78	8	843	2941.34	3.49	1.4303
28	16.4900	961.68	8	843	2933.44	3.48	1.4282
29	17.1704	1045.44	9	742	2849.68	3.84	1.6465
30	17.9900	1077.10	9	742	2818.02	3.80	1.6044
31	18.2609	1125.00	9	742	2770.12	3.73	1.5967
32	18.9511	1181.76	9	742	2713.36	3.66	1.5834

Table 3.1.1 - Variable Flow-rate Drawdown Data.

Σ	ABS (Σ)	$\Delta P'$, psi/hr	ABS($\Delta P'$), psi/hr
12244.9	12244.9	4791.05	4791
1224.0	1224.0	1314.29	1314
660.0	660.0	384.91	385
378.0	378.0	169.28	169
351.7	351.7	163.87	164
313.8	313.8	143.26	143
160.0	160.0	53.25	53
78.5	78.5	-15.22	15
0.0	0.0	0.00	0
-11.6	11.6	-67.18	67
74.4	74.4	15.08	15
0.0	0.0	0.00	0
-33.6	33.6	-63.36	63
-2.2	2.2	-27.42	27
0.0	0.0	0.00	0
-17.6	17.6	-38.38	38
0.0	0.0	0.00	0
0.0	0.0	0.00	0
0.0	0.0	0.00	0

Table 3.1.2 - $\Delta P'_{wf}$, psi/hr and Σ Data

n	t,hr	P _{wf} , psi	ΔP , psi	Δt , hr	$\Delta P'$, psi/hr	$t^* \Delta P'$, psi	X	X'	abs X'
1	0.000	2857	0	0					
2	1.000	3143	286	1					
3	2.000	3180	323	2	25.500	51.00	3.6010	-0.2849	0.2849
4	3.000	3194	337	3	11.000	33.00	3.5006	-0.1899	0.1899
5	4.000	3202	345	4	6.6667	26.67	3.4295	-0.1424	0.1424
6	6.000	3210	353	6	3.7500	22.50	3.3293	-0.0948	0.0948
7	8.000	3217	360	8	2.5000	20.00	3.2582	-0.0711	0.0711
8	10.00	3220	363	10	2.0000	20.00	3.2031	-0.0568	0.0568
9	12.00	3225	368	12	2.1667	26.00	3.1581	-0.0473	0.0473
10	15.00	3230	373	15	1.5000	22.50	3.1030	-0.0378	0.0378
11	18.00	3234	377	18	1.4048	25.29	3.0581	-0.0315	0.0315
12	22.00	3240	383	22	0.0000		3.0087	0.0000	0.0000

Table 3.2 - Two-Rate Test Data

n	t, hrs	Pwf, psia	q, (STB/D)	ΔP , psi	$\Delta P/q$, psi/STB	Xn	teq, hr	$(\Delta P/q)'$, psi/STB	$t^*(\Delta P/q)'$, psi/STB
1	0.000	5000	0	0.0	0.0000				
2	0.114	4927	145	73.0	0.5034	-0.943	0.114	3.64712	0.4158
3	0.136	4917	143	83.0	0.5804	-0.855	0.140	3.35147	0.4558
4	0.164	4905	142	95.0	0.6690	-0.772	0.169	2.96151	0.4857
5	0.197	4893	141	107.0	0.7589	-0.691	0.204	2.54586	0.5015
6	0.236	4881	140	119.0	0.8500	-0.611	0.245	2.30488	0.5440
7	0.283	4868	138	132.0	0.9565	-0.525	0.298	1.99199	0.5637
8	0.340	4856	137	144.0	1.0511	-0.446	0.358	1.54612	0.5257
9	0.408	4844	136	156.0	1.1471	-0.367	0.429	1.26892	0.5177
10	0.490	4833	135	167.0	1.2370	-0.288	0.516	1.03756	0.5084
11	0.587	4823	133	177.0	1.3308	-0.203	0.627	0.80094	0.4702
12	0.705	4815	132	185.0	1.4015	-0.125	0.750	0.50869	0.3586
13	0.846	4809	131	191.0	1.4580	-0.046	0.898	0.37921	0.3208
14	1.020	4804	129	196.0	1.5194	0.040	1.097	0.27073	0.2761
15	1.220	4801	128	199.0	1.5547	0.116	1.307	0.14930	0.1822
16	1.460	4799	127	201.0	1.5827	0.193	1.560	0.09582	0.1399
17	1.750	4798	126	202.0	1.6032	0.271	1.867	0.08119	0.1421
18	2.110	4797	124	203.0	1.6371	0.358	2.281	0.06536	0.1379
19	2.530	4797	123	203.0	1.6504	0.435	2.721	0.02957	0.0748
20	3.030	4797	122	203.0	1.6639	0.512	3.250	0.02502	0.0758
21	3.640	4797	121	203.0	1.6777	0.591	3.897	0.02462	0.0896
22	4.370	4798	119	202.0	1.6975	0.676	4.746	0.02229	0.0974
23	5.240	4798	118	202.0	1.7119	0.753	5.659	0.01167	0.0611
24	6.290	4799	117	201.0	1.7179	0.831	6.771	0.00879	0.0553
25	7.500	4799	116	201.0	1.7328	0.907	8.064	0.01547	0.1160
26	9.050	4799	114	201.0	1.7632	0.994	9.866	0.01234	0.1116
27	10.900	4800	113	200.0	1.7699	1.072	11.81	0.00347	0.0379
28	13.000	4801	112	199.0	1.7768	1.148	14.05	0.00736	0.0957
29	15.600	4801	110	199.0	1.8091	1.233	17.11	0.00790	0.1232
30	18.800	4802	109	198.0	1.8165	1.311	20.47	0.00219	0.0412
31	22.500	4803	108	197.0	1.8241	1.388	24.42	0.00283	0.0637
32	27.000	4803	107	197.0	1.8411	1.472	29.64	0.00422	0.1138
33	32.400	4804	105	196.0	1.8667	1.575	37.62	0.00317	0.1026
34	38.900	4805	104	195.0	1.8750	1.669	46.63	0.00119	0.0465
35	46.700	4806	103	194.0	1.8835	1.765	58.16	0.00101	0.0473
36	56.100	4807	102	193.0	1.8922	1.864	73.04	0.00204	0.1146
37	67.300	4807	100	193.0	1.9300	1.984	96.39	0.00216	0.1453
38	80.700	4808	99	192.0	1.9394	2.088	122.56	0.00065	0.0526
39	96.900	4809	98	191.0	1.9490	2.196	156.95		

Table 3.3 - Data for Three and Multi-Rate Test.

Analysis Techniques	Parameters	
	Permeability, K (md)	Skin Factor, S
Superposition Time Cartesian Plot	11.16	4.03
Equivalent Time Semi-Log Plot	11.15	4.02
Tiab's Direct Synthesis	11.19	4.19

Table 4.1 - Comparison of Results Estimated by Different Techniques for Continuously Changing Flowrates.

Analysis Techniques	Parameters	
	Permeability, K (md)	Skin Factor, S
Constant Rate Cartesian Plot Pressure Function	19.12	-3.20
Constant Rate Semi-Log Plot Pressure Function	19.36	-3.97
Constant Rate Cartesian Plot Pressure Derivative	21.32	-3.23

Table 4.2 - Comparison of Results Estimated by Different Techniques for Constant Flowrates.

Analysis Techniques	Parameters	
	Permeability, K (md)	Skin Factor, S
Cartesian Plot Pressure Function	12.63	0.8
Cartesian Plot Pressure Derivative	12.50	-
Log-Log Plot Tiab's Direct Synthesis	12.96	0.9

Table 4.3 - Comparison of Results Estimated by Different Techniques for Two-Rates Test.